A73L174 R.O.1

Copy 44
RM SL55I22

[redacted]

R.A. A73L174 R.O.1

UNCLASSIFIED

NACA

RESEARCH MEMORANDUM

for the

U. S. Air Force

AERODYNAMIC CHARACTERISTICS OF A 0.04956-SCALE

MODEL OF THE CONVAIR F-102A AIRPLANE AT MACH

NUMBERS OF 1.41, 1.61, AND 2.01

By M. Leroy Spearman and Cornelius Driver

Langley Aeronautical Laboratory
Langley Field, Va.

CLASSIFICATION CHANGED
UNCLASSIFIED

To ____

By authority of TPA #63 Date Effective 12/1/61

CLASSIFIED DOCUMENT

NATIONAL ADVISORY COMMITTEE FOR AERONAUTICS

WASHINGTON

[redacted]

UNCLASSIFIED

UNCLASSIFIED

NACA RM SL55I22

[redacted]

NATIONAL ADVISORY COMMITTEE FOR AERONAUTICS

RESEARCH MEMORANDUM

for the

U. S. Air Force

AERODYNAMIC CHARACTERISTICS OF A 0.04956-SCALE MODEL OF THE CONVAIR F-102A AIRPLANE AT MACH NUMBERS OF 1.41, 1.61, AND 2.01

By M. Leroy Spearman and Cornelius Driver

SUMMARY

Tests have been made in the Langley 4- by 4-foot supersonic pressure tunnel at Mach numbers of 1.41, 1.61, and 2.01 of various arrangements of a 0.04956-scale model of the Convair F-102A airplane with faired inlets. Tests were made of the model equipped with a plain wing, a wing with 6.4 percent conical camber, and a wing with 15 percent conical camber. Body modifications including an extended nose, a modified canopy, and extended afterbody fillets were evaluated. In addition, the effects of a revised vertical tail and two different ventral fins were determined.

The results indicated that the use of cambered wings resulted in lower drag in the lift-coefficient range above about 0.2. This range, however, is above that which would generally be required for level flight; hence, the usefulness of camber might be confined to increased maneuverability at the higher lifts while its use may be detrimental to the high-speed (low-lift) capabilities.

Neutral directional stability for the basic configuration (6.4 percent camber) occurred at an angle of attack of 12.6° for a Mach number of 1.41 and at 7° for a Mach number of 2.01. Increasing the camber to 15 percent resulted in a further decrease in the angle of attack from 7° to 6° for neutral stability at a Mach number of 2.01.

The directional characteristics were improved slightly by the use of ventral fins and were further improved by the use of a revised vertical tail to the extent that neutral directional stability for the 15-percent cambered configuration at a Mach number of 2.01 was delayed from an angle of attack of 6° to 9.6°.

[redacted]

UNCLASSIFIED

INTRODUCTION

At the request of the U. S. Air Force, the National Advisory Committee for Aeronautics has undertaken an investigation of the aerodynamic characteristics of the Convair F-102A airplane in the Langley 4- by 4-foot supersonic pressure tunnel at $M = 1.41$, 1.61, and 2.01.

Tests of various arrangements of the F-102 configuration that have previously been made in the same tunnel include the following: the basic YF-102 configuration (ref. 1), the YF-102 with various extended afterbodies (ref. 2), and the revised YF-102 configuration having an extended contoured afterbody with both an uncambered wing and a 6.4-percent conically cambered wing with 10^{o} reflexed tips (ref. 3). The basic F-102A configuration, for which results are presented herein, retains the body contouring and the 6.4-percent cambered wing and reflexed tips of the last previous configuration (ref. 3) but differs in the following respects: a modified canopy, an extended nose, and extended afterbody fillets. The tests were made with the inlets faired closed.

In addition to the results for the basic configuration, results are presented herein for the configuration having an uncambered wing, a wing with 15 percent conical camber, a revised vertical tail, and two ventral fins.

SYMBOLS

The results are presented as standard NACA coefficients of forces and moments. The data are referred to the stability-axis system (fig. 1) with the reference center of moments located at 25 percent of the wing mean geometric chord. The coefficients are based on the geometric characteristics of the wing with 15 percent conical camber.

The symbols are defined as follows:

C_L lift coefficient, $-Z/qS$

C_X longitudinal-force coefficient, X/qS (equal and opposite to drag coefficient at $\beta = 0^{o}$)

C_Y lateral-force coefficient, Y/qS

C_n yawing-moment coefficient, N/qSb

C_l rolling-moment coefficient, L'/qSb

C_m — pitching-moment coefficient, $M'/qS\bar{c}$

Z — force along Z-axis

X — force along X-axis

Y — force along Y-axis

N — moment about Z-axis

L' — moment about X-axis

M' — moment about Y-axis

L — lift (-Z)

D — drag (-X at $B = 0^{\circ}$)

q — free-stream dynamic pressure

S — wing area including body intercept, 1.732 sq ft

b — wing span, 24.758 in.

$\bar{c}$ — wing mean geometric chord, 13.43 in.

M — Mach number

T.E. — trailing edge

α — angle of attack, deg

β — angle of sideslip, deg

δ_e — elevon deflection, deg

$\partial C_m/\partial C_L$ — variation of pitching-moment coefficient with lift coefficient at $C_m = 0$ (measure of margin of static longitudinal stability)

C_{m_o} — pitching-moment coefficient at $C_L = 0$

$\alpha_{C_L=0}$ — angle of attack for $C_L = 0$

C_{L_α} — lift-curve slope, $\partial C_L/\partial_\alpha$ at $C_L = 0$

[redacted]

L/D lift-drag ratio

$\Delta C_X / C_L^2$ drag-due-to-lift parameter

C_{n_β} variation of yawing-moment coefficient with sideslip angle (static directional stability derivative), $\partial C_n / \partial \beta$ at $\beta = 0$

C_{l_β} variation of rolling-moment coefficient with sideslip angle (effective-dihedral derivative), $\partial C_l / \partial \beta$ at $\beta = 0$

C_{Y_β} variation of lateral-force coefficient with sideslip angle, $\partial C_Y / \partial \beta$ at $\beta = 0$

MODEL AND APPARATUS

A three-view drawing of the 0.04956-scale Convair F-102A configuration indicating the body and canopy revisions is shown in figure 2. The geometric characteristics of the model are presented in table I. The model has a basic 60° delta wing mounted on the fuselage in a mid-low position. The basic vertical tail is similar in plan form to the wing semispan. Twin ram-type inlets are located well forward on the sides of the fuselage, but for the present tests the inlets were closed by means of faired plugs.

A comparison of the revised vertical tail and the basic vertical tail is shown in figure 3. Details of the two ventral fins investigated are shown in figure 4. Photographs of the model are shown in figure 5.

The wing with 6.4 percent conical camber was designed for a lift coefficient of 0.15 at $M = 1.0$ and had, in addition to the camber, a 10° upward deflection of the trailing-edge portion outboard of the elevons. The wing with 15 percent conical camber was designed for a lift coefficient of 0.21 at $M = 1.0$. The portions of the trailing edge outboard of the elevons for this wing were deflected upward to an angle that varied linearly from 9° at the inboard end to 5° at the outboard end.

Forces and moments were measured by means of a six-component internal strain-gage balance and indicating system.

TESTS AND CORRECTIONS

Test Conditions

The tests were made at Mach numbers of 1.41, 1.61, and 2.01 for which the Reynolds numbers (based on $\bar{c}$) are 3.41×10^6, 3.26×10^6, and 2.82×10^6, respectively. The stagnation dewpoint was maintained at -25° F or less, so that no condensation effects were encountered in the test section.

Pitch tests were made through an angle-of-attack range from about -2° to about 13°. Sideslip tests were made through a sideslip-angle range from about -4° to 10°. Sideslip tests were made at $\alpha = 1.5^\circ$ and $\alpha = 5.6^\circ$. In addition, pitch tests were made at $\beta = 4^\circ$ in order to obtain an indication of angle-of-attack effects on the sideslip derivatives.

Corrections and Accuracy

The angles of attack and sideslip have been corrected for the deflections of the sting and balance due to the aerodynamic loads. The base pressure was measured and the longitudinal-force coefficient was adjusted to correspond to a base pressure equal to free-stream static pressure.

The estimated errors in the individual measured quantities are as follows:

C_L	± 0.006
C_X	± 0.001
C_m	± 0.002
C_l	± 0.0004
C_n	± 0.0002
C_Y	± 0.004
α, deg	± 0.1
β, deg	± 0.1
δ_e, deg	± 0.1

RESULTS AND DISCUSSION

Longitudinal Characteristics

Effects of wing camber.- The effects of wing camber on the aerodynamic characteristics in pitch at Mach numbers of 1.41, 1.61, and 2.01 are presented in figure 6 and the variations of the various longitudinal parameters with Mach number are summarized in figure 7. The primary advantage of the increased camber, of course, is to reduce progressively the drag due to lift $\Delta C_X/C_L^2$, and to increase slightly the lift-curve slope C_{L_α}. The use of 6.4 percent camber results in a reduction in the stability $-\frac{\partial C_m}{\partial C_L}$ and produces a positive shift in C_{m_o}, so that the control deflection required for trim, and thus the drag-due-to-trim, should be reduced. No such positive shift in C_{m_o} occurred for the wing with 15 percent camber and the stability was slightly greater than that for the plain wing.

The advantages of camber at higher lifts are, however, offset in the low-lift high-speed range by an increase in drag. Near zero lift, for example, $C_{X_{min}}$ for the 15-percent cambered wing is about 0.005 greater than that for the plain wing. In fact, the advantages of camber in reducing drag are realized only in the lift range above about 0.2 which would generally be beyond that required for level flight in the Mach number range from 1.4 to 2.0. Hence, the usefulness of camber in this Mach number range may be confined to increased maneuverability resulting from lower drag at the higher lifts, whereas, for the probable level-flight lift range the use of camber may be a detriment to the high-speed capabilities.

There is little effect of camber on the maximum lift-drag ratio $(L/D)_{max}$ but the lift coefficient at which the maximum L/D occurs is, in general, increased with increasing camber.

Effects of elevon deflection.- The effects of elevon deflection on the aerodynamic characteristics in pitch were determined only for the configuration with 6.4 percent camber and for a Mach number of 2.01 (see fig. 8). The longitudinal trim characteristics for this configuration are summarized in figure 9.

The control deflection for trim and the trim angle of attack vary in an essentially linear manner with lift coefficient. A maximum lift coefficient of 0.135 was obtained with the maximum control deflection investigation (-15°). As a result of the drag due to trim, the maximum L/D obtained was about 3.5 compared to about 4.5 for the same lift coefficient with undeflected controls.

Effects of vertical tail.- A comparison of the aerodynamic characteristics in pitch with the basic and the revised vertical tail (fig. 10) indicates no significant difference with the possible exception of a slightly higher minimum drag with the revised vertical tail.

Effects of body modifications.- The effects of the body modifications are presented in figure 11 for Mach numbers of 1.41 and 2.01. The revised F-102A modifications include a new canopy, an extended nose, and an extended afterbody fillet. The primary effect of the body modifications, as might be expected, is to reduce the drag. The minimum drag coefficient at $M = 1.41$ was reduced from 0.028 to 0.023 and at $M = 2.01$ was reduced from 0.024 to 0.022.

Lateral and Directional Characteristics

Effects of sideslip.- The aerodynamic characteristics in sideslip at $\alpha = 1.5^{\circ}$ for Mach numbers of 1.61 and 2.01 for the configuration with 6.4 percent camber (figs. 12 and 13) indicate fairly linear characteristics to a sideslip angle of about 4°. At $\alpha = 5.7^{\circ}$ for $M = 2.01$ (fig. 14) the basic configuration is essentially neutrally stable to $\beta \approx 6^{\circ}$ and then becomes directionally unstable. The addition of the large ventral fin to this configuration is sufficient to increase the yawing moment throughout the sideslip range so that unstable moments are forestalled to $\beta \approx 10^{\circ}$.

The effects of wing camber on the aerodynamic characteristics in sideslip at $\alpha = 5.6$ and $M = 2.01$ for the tail-off configuration (fig. 15) indicate that increasing the camber from 6.4 percent to 15 percent results in a slight increase in directional instability and an increase in the negative dihedral effect C_{l_β}.

Effects of angle of attack.- The effects of angle of attack on the sideslip characteristics in the linear sideslip range ($\beta = 4^{\circ}$) are presented for the various configurations and Mach numbers in figures 16 through 21. At $M = 1.41$ the basic configuration with 6.4 percent camber (figs. 16 and 17) indicates a progressive decrease in directional stability with increasing angle of attack until neutral directional stability occurs at $\alpha \approx 12.6^{\circ}$. The configuration with the revised vertical tail maintained directional stability to the highest angle of attack obtained (12.6°). Of course, the rolling-moment and lateral-force variations with sideslip angle are also increased for the revised vertical-tail configuration.

For a Mach number of 2.01 (figs. 18 and 19) the directional stability decreases progressively with increasing angle of attack until neutral directional stability occurs at $\alpha \approx 7^{\circ}$. The level of directional stability is increased slightly with the addition of the small ventral fin, and is increased still further with the large ventral fin so that neutral stability occurs at $\alpha \approx 10.3^{\circ}$.

The results obtained at $M = 2.01$ for the 15-percent cambered configuration (figs. 20 and 21) indicate a greater decrease in directional stability with increasing angle of attack so that for the basic vertical tail neutral stability occurs at $\alpha \approx 6^{\circ}$ compared to $\alpha \approx 7^{\circ}$ for the 6.4-percent cambered configuration. The revised vertical tail for the 15-percent cambered configuration increases the directional stability to the extent that neutral stability does not occur until $\alpha \approx 9.6^{\circ}$.

The decrease in directional stability with increasing angle of attack occurs primarily as a result of a decreased tail effectiveness as indicated by the convergence of the C_{Y_β} and C_{n_β} curves with increasing angle of attack (figs. 17, 19, and 21) for the tail-on and tail-off configurations. In addition, the slightly greater decrease in C_{n_β} with angle of attack indicated for the 15-percent cambered configuration apparently occurs as a result of an increase in the unstable moment of the tail-off configuration with increasing angle of attack that is more significant than for the 6.4-percent cambered configuration.

A summary of the variation of the sideslip derivatives with Mach number at $\alpha = 1.5^{\circ}$ for the 6.4-percent cambered configuration with various tail arrangements is presented in figure 22.

CONCLUSIONS

Tests of various arrangements of a model of the Convair F-102A airplane with faired inlets at Mach numbers of 1.41, 1.61, and 2.01 indicated the following conclusions:

1. The use of cambered wings resulted in lower drag in the lift-coefficient range above that which would generally be required for level flight (about 0.2); hence, the usefulness of camber may be confined to increased maneuverability at the higher lifts while its use may be detrimental to the high-speed (low-lift) capabilities.

2. The addition of an extended nose, an improved canopy, and an extended afterbody fillet caused a reduction in drag coefficient at a Mach number of 1.41 from 0.028 to 0.023 and at a Mach number of 2.01 from 0.024 to 0.022.

3. Neutral directional stability for the basic configuration (6.4 percent camber) occurred at an angle of attack of 12.6° for a Mach number of 1.41 and at an angle of attack of 7° for a Mach number of 2.01.

4. Increasing the wing camber to 15 percent resulted in a slightly greater decrease in directional stability with increasing angle of attack so that at a Mach number of 2.01 the angle of attack for neutral directional stability was reduced from 7° to 6°.

5. The directional characteristics were improved slightly by the use of ventral fins and were improved by the use of a revised vertical tail to the extent that neutral directional stability for the configuration having 15 percent camber was delayed from an angle of attack of 6° to 9.6° at a Mach number of 2.01.

Langley Aeronautical Laboratory,
National Advisory Committee for Aeronautics,
Langley Field, Va., September 16, 1955.

M. Leroy Spearman
M. Leroy Spearman
Aeronautical Research Scientist

Cornelius Driver
Cornelius Driver
Aeronautical Research Scientist

Approved: John V. Becker
John V. Becker
Chief of Compressibility Research Division

rmw

REFERENCES

1. Hilton, John H., Jr., Hamilton, Clyde V., and Lankford, John L.: Preliminary Wind-Tunnel Investigation of a 1/20-Scale Model of the Convair MX-1554 at Mach Numbers of 1.61 and 2.01. NACA RM SL52L11a, U. S. Air Force, 1952.

2. Hilton, John H., Jr., and Palazzo, Edward B.: Wind-Tunnel Investigation of a Modified 1/20-Scale Model of the Convair MX-1554 Airplane at Mach Numbers of 1.41 and 2.01. NACA RM SL53G30, U. S. Air Force, 1953.

3. Spearman, M. Leroy, and Hughes, William C.: Aerodynamic Characteristics at a Mach Number of 1.41 of a Model of the Convair F-102 Airplane Equipped With an Extended Contoured Afterbody, Cambered Wing Leading Edge, and Reflexed Wing-Tip Trailing Edge. NACA RM SL54J26, U. S. Air Force, 1954.

[redacted]

TABLE I

GEOMETRIC CHARACTERISTICS OF MODEL

Wing	6.4 percent camber	15.0 percent camber
Area, sq ft	1.715	1.732
Span, in.	23.196	24.758
Mean geometric chord, in.	13.75	13.43
Aspect ratio	2.189	2.458
Taper ratio	0	0
Airfoil section	NACA 0004-65 (mod.)	NACA 0004-63 (mod.)
Angle of incidence, deg	0	0
Dihedral angle, deg	0	0
Sweep of leading edge, deg	60.1	57
Sweep of trailing edge, deg	-5	-5

Vertical tail	Basic	Revised
Area (exposed), sq in.	24.20	25.45
Span to body center line, in. . . .	6.79	6.86
Aspect ratio	2	2
Taper ratio	0	0.19
Airfoil section	NACA 0004-65 (mod.)	Modified hexagon
Sweep of leading edge, deg	60	60
Sweep of trailing edge, deg	-5	20

[redacted]

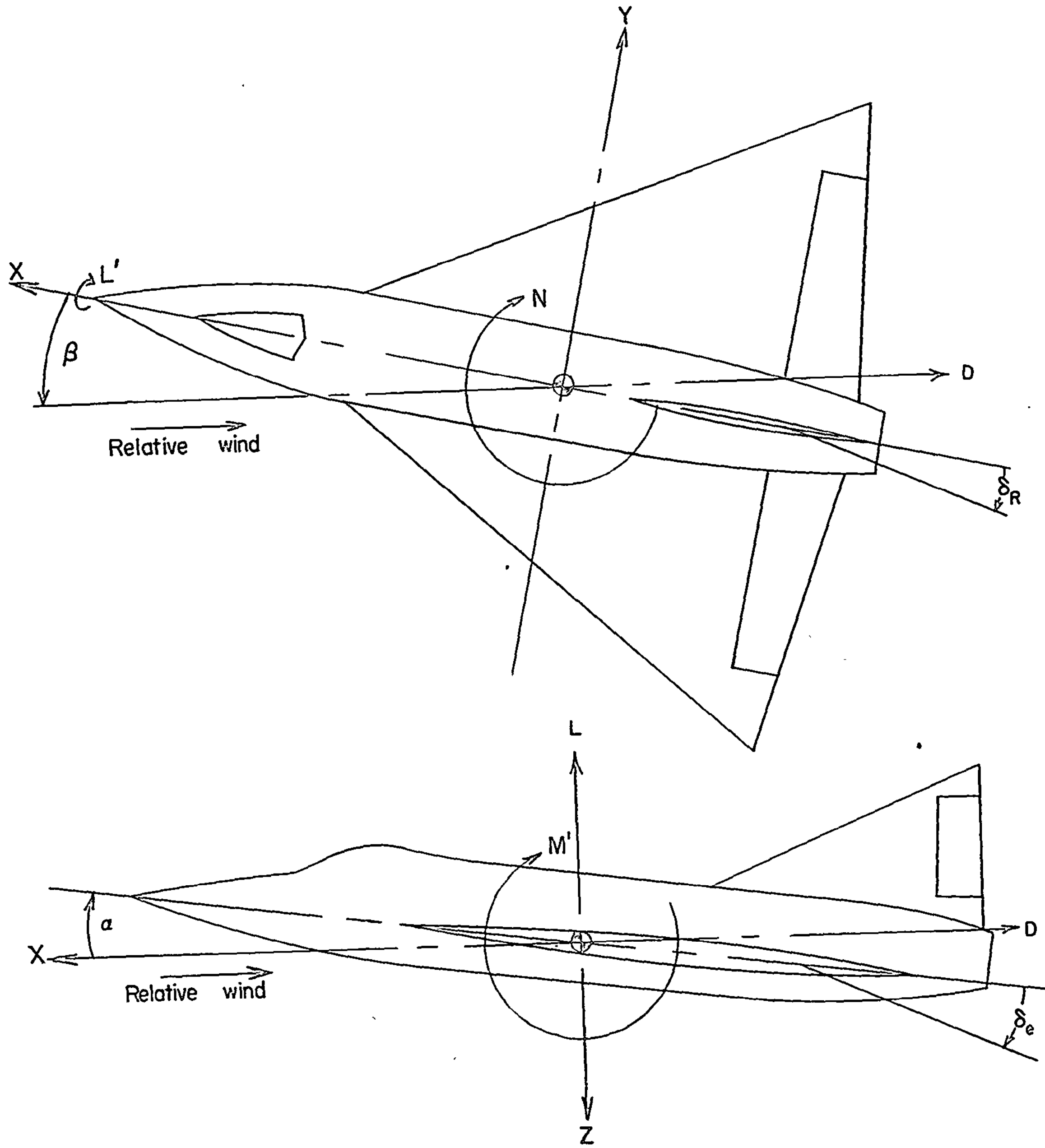

Figure 1.- System of stability axes.

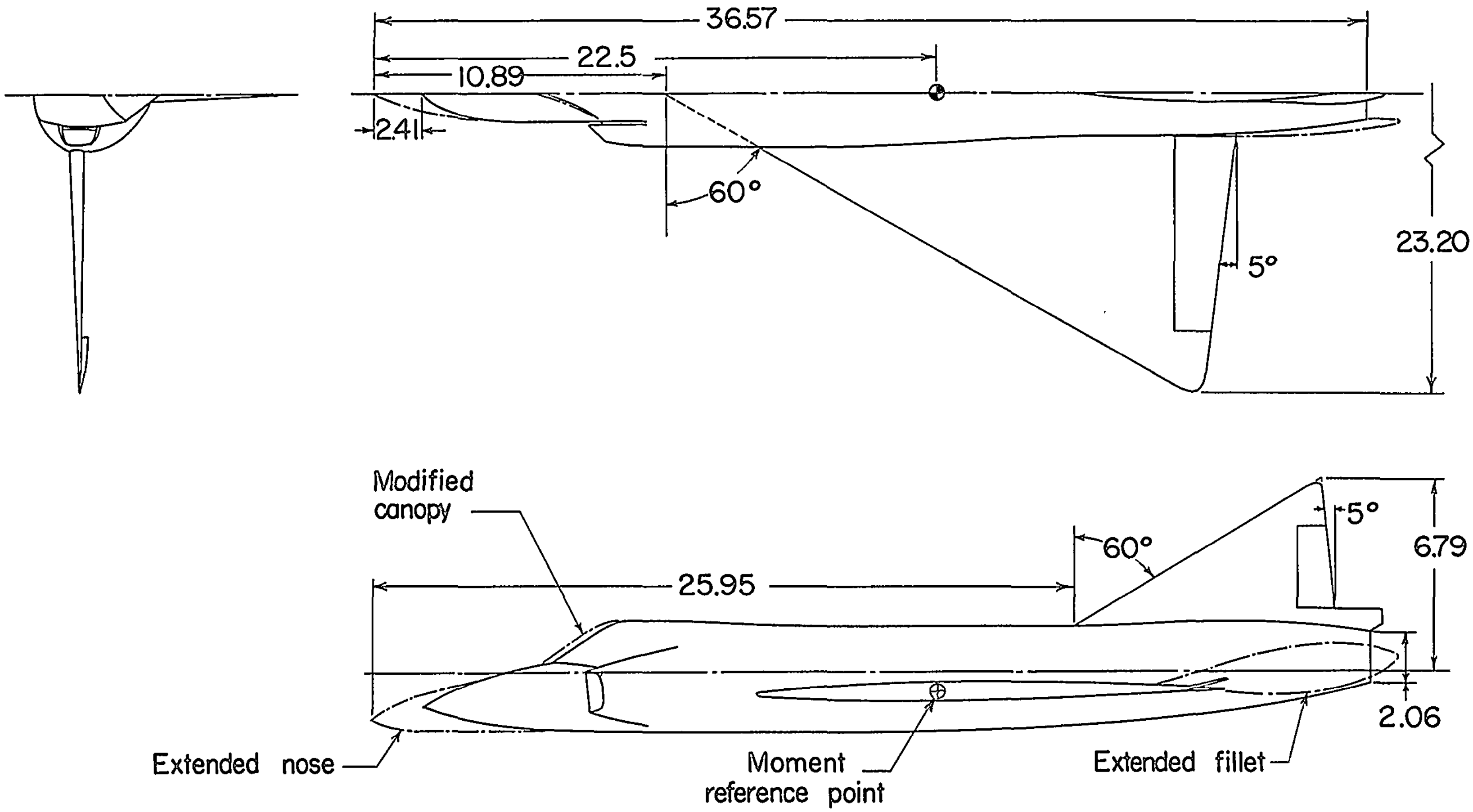

Figure 2.- Details of 0.04956-scale Convair F-102A configuration.

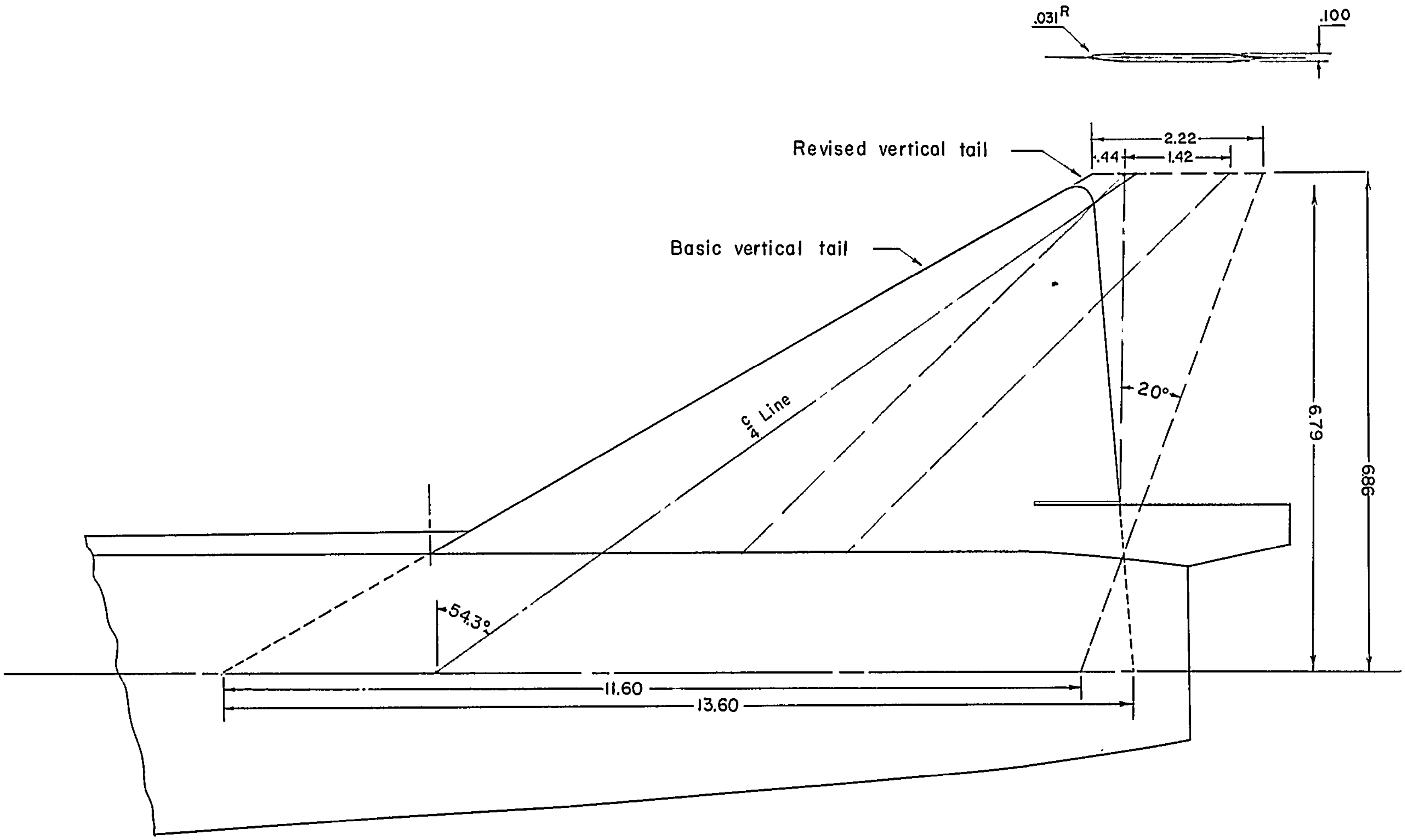

Figure 3.- Details of revised vertical tail.

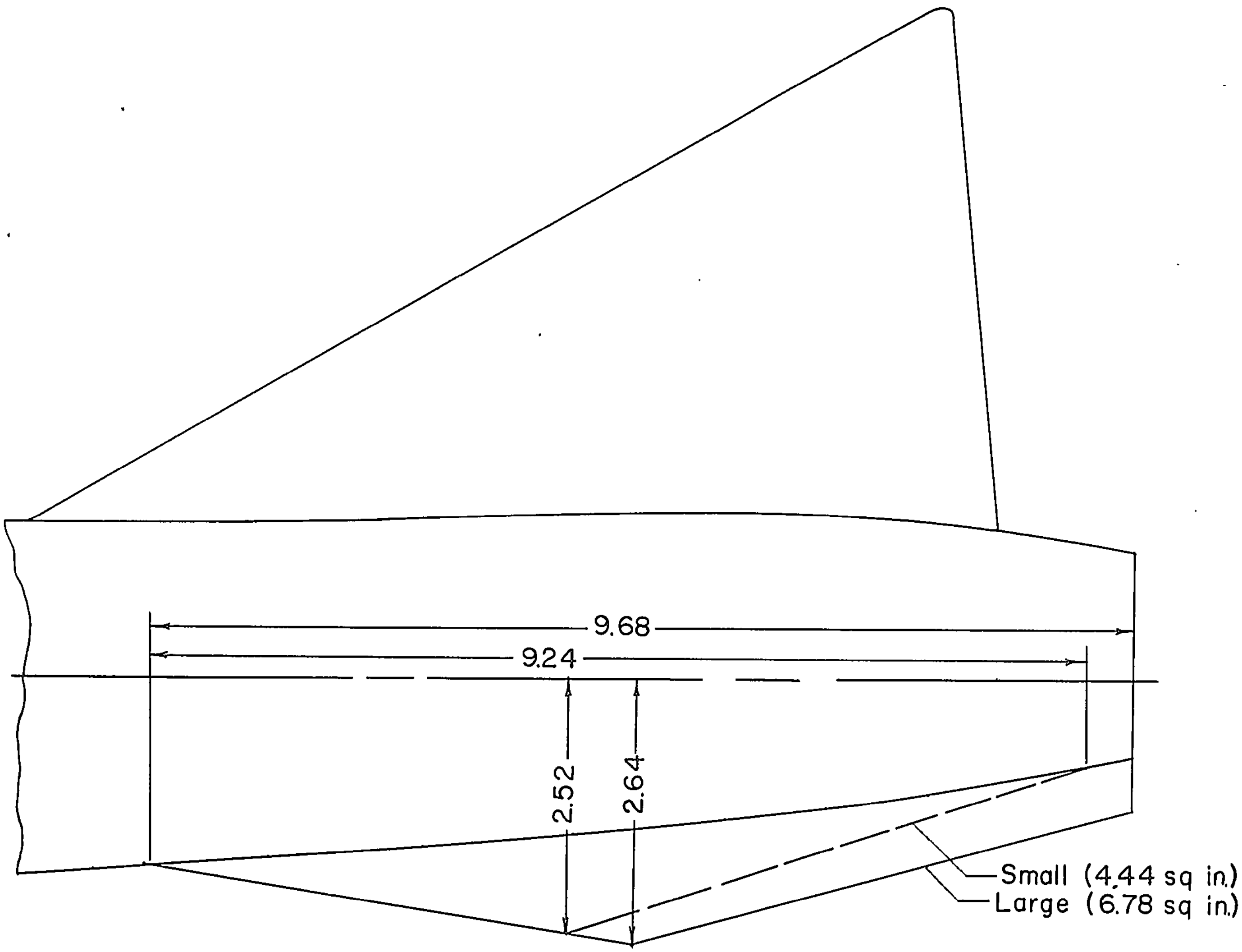

Figure 4.- Details of ventral fins.

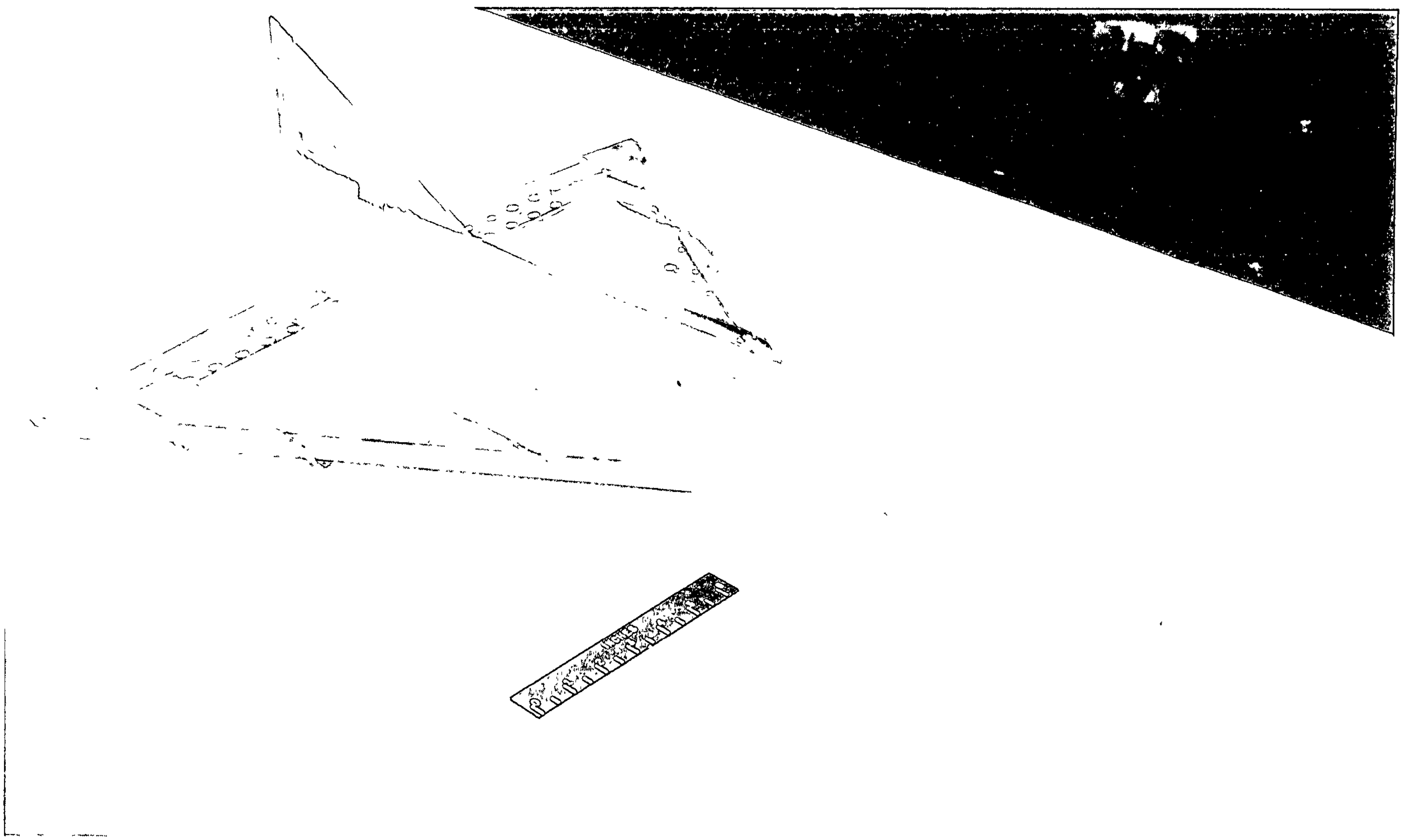

L-87819

(a) Basic vertical tail.

Figure 5.- Photographs of model.

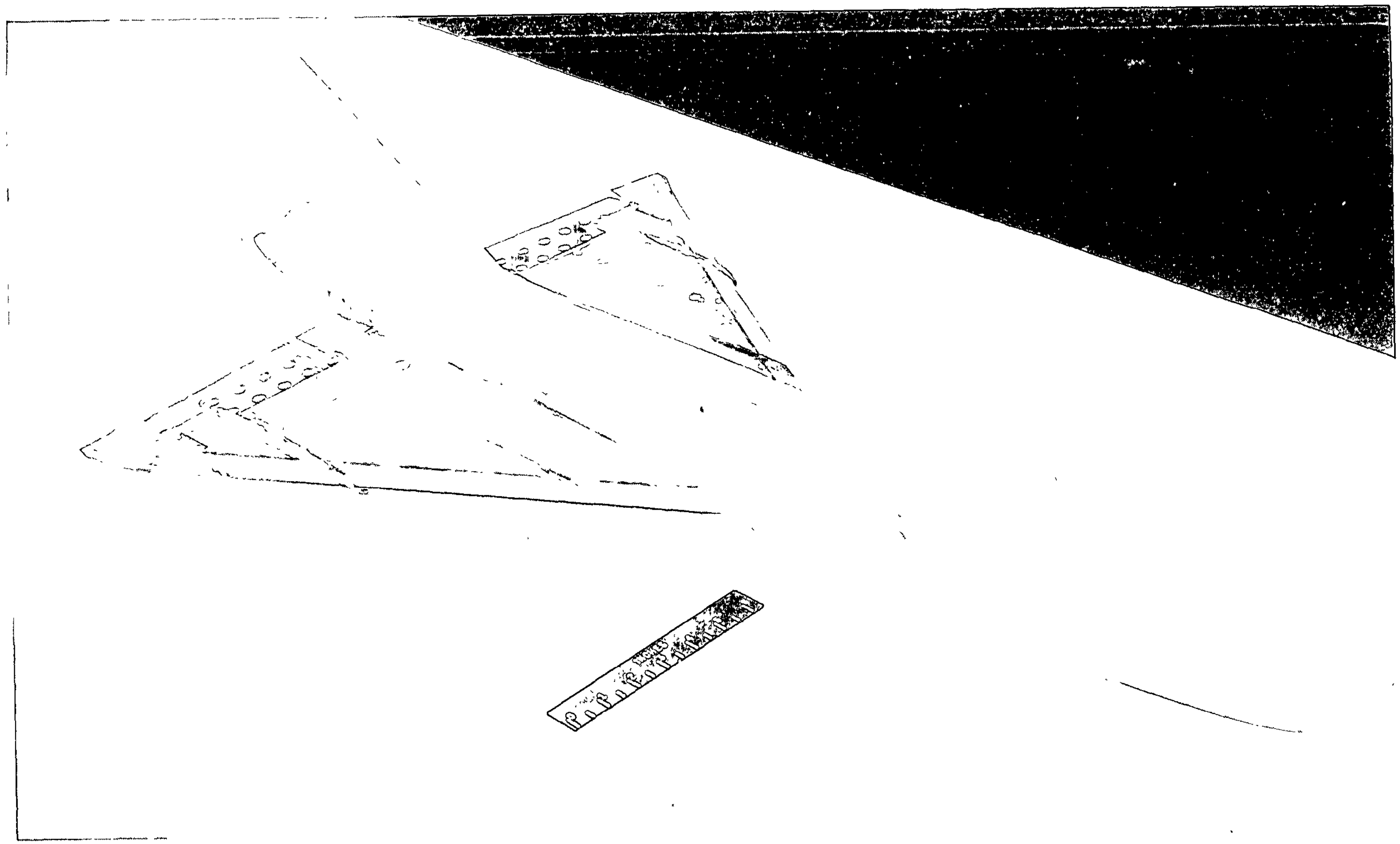

L-87818

(b) Revised vertical tail.

Figure 5.- Concluded.

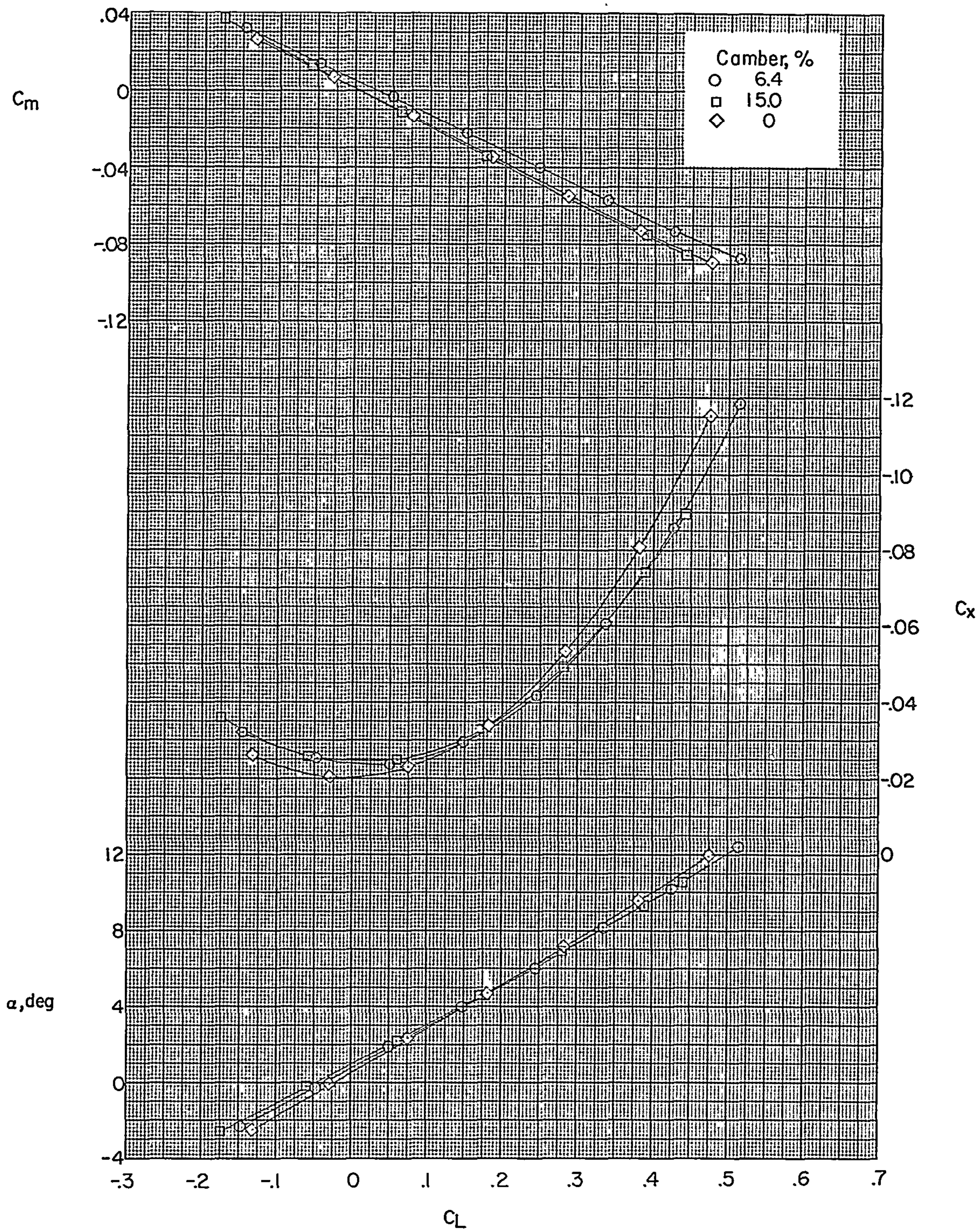

(a) M = 1.41.

Figure 6.- Effects of wing camber on aerodynamic characteristics in pitch.

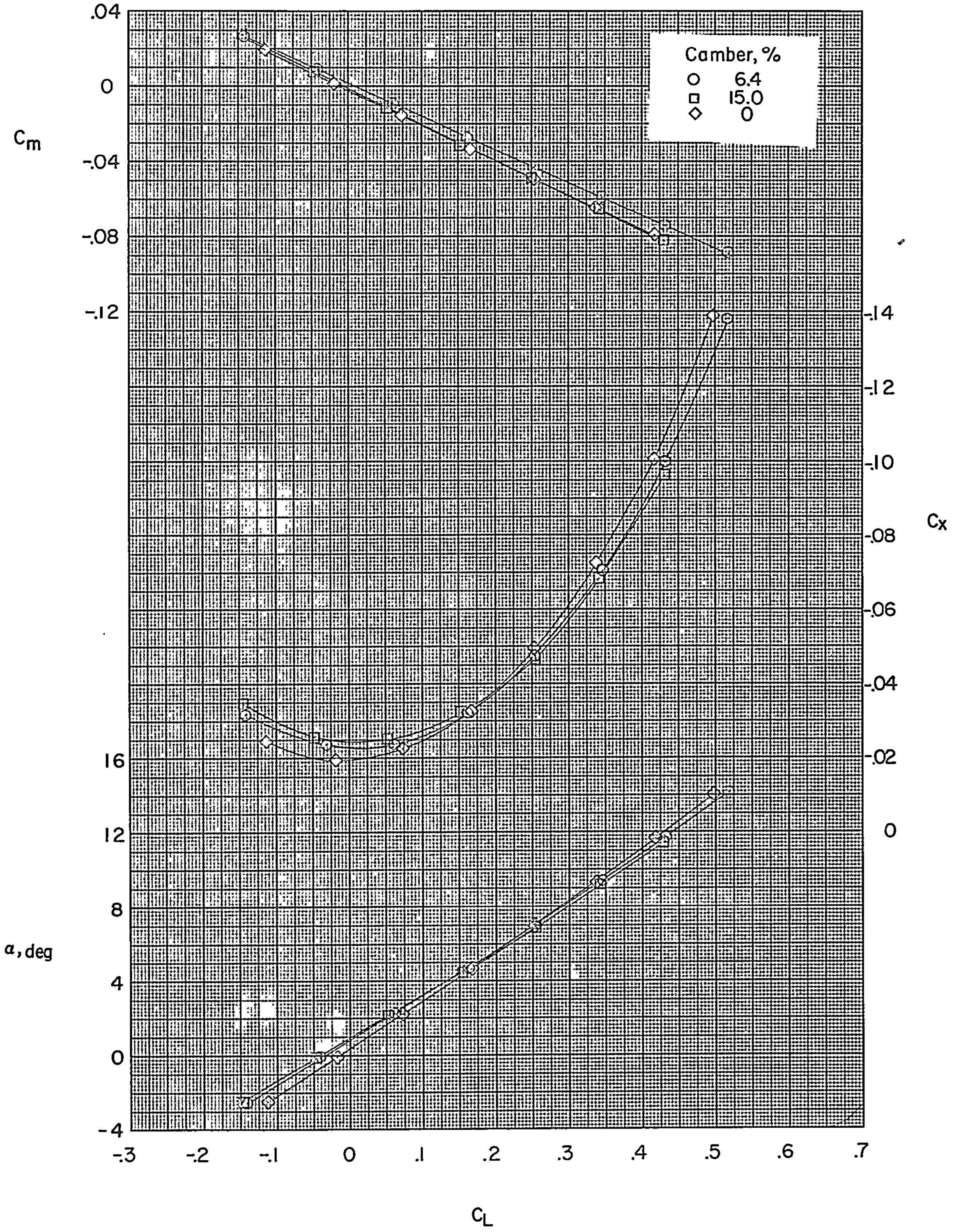

(b) M = 1.61.

Figure 6.- Continued.

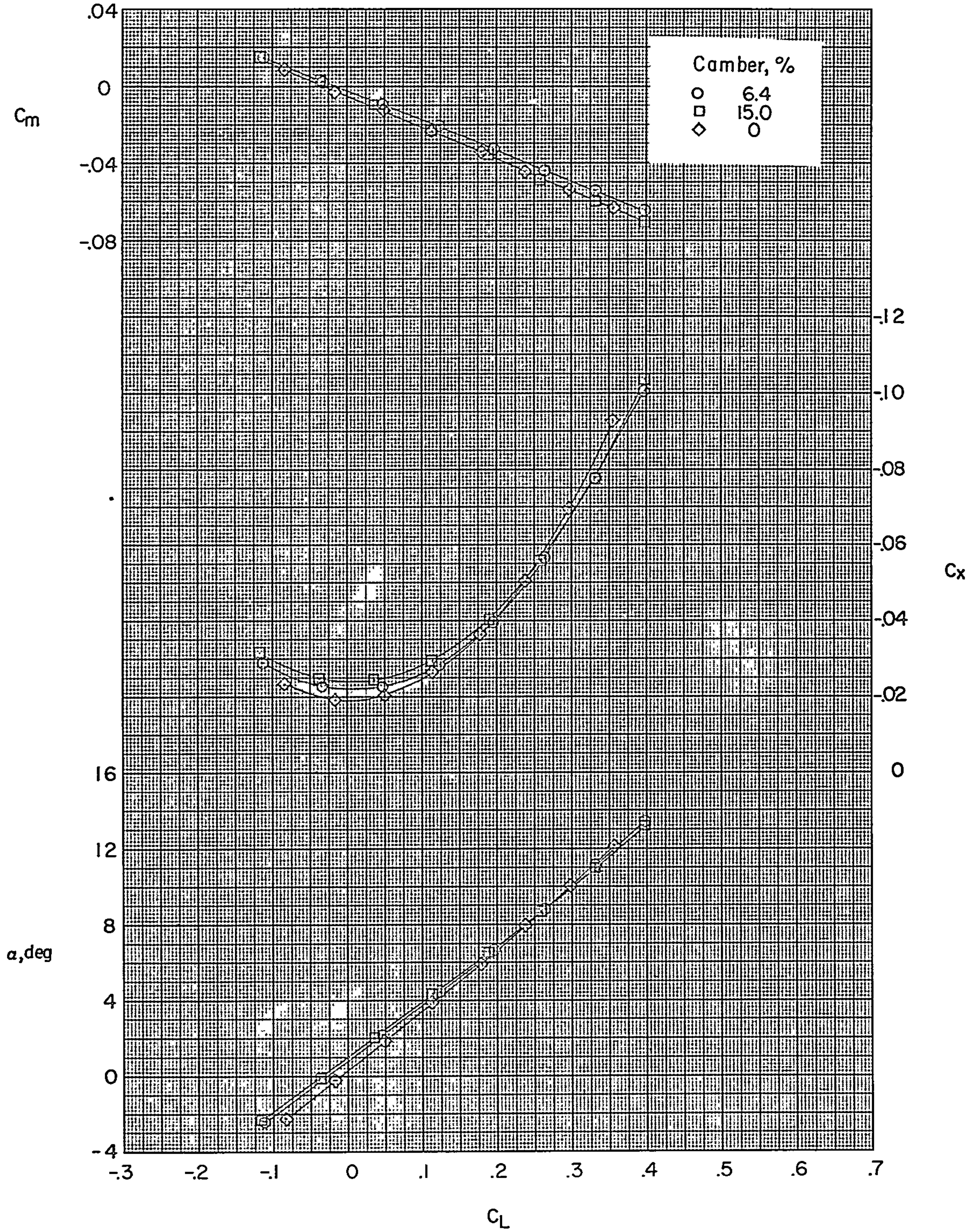

(c) M = 2.01.

Figure 6.- Concluded.

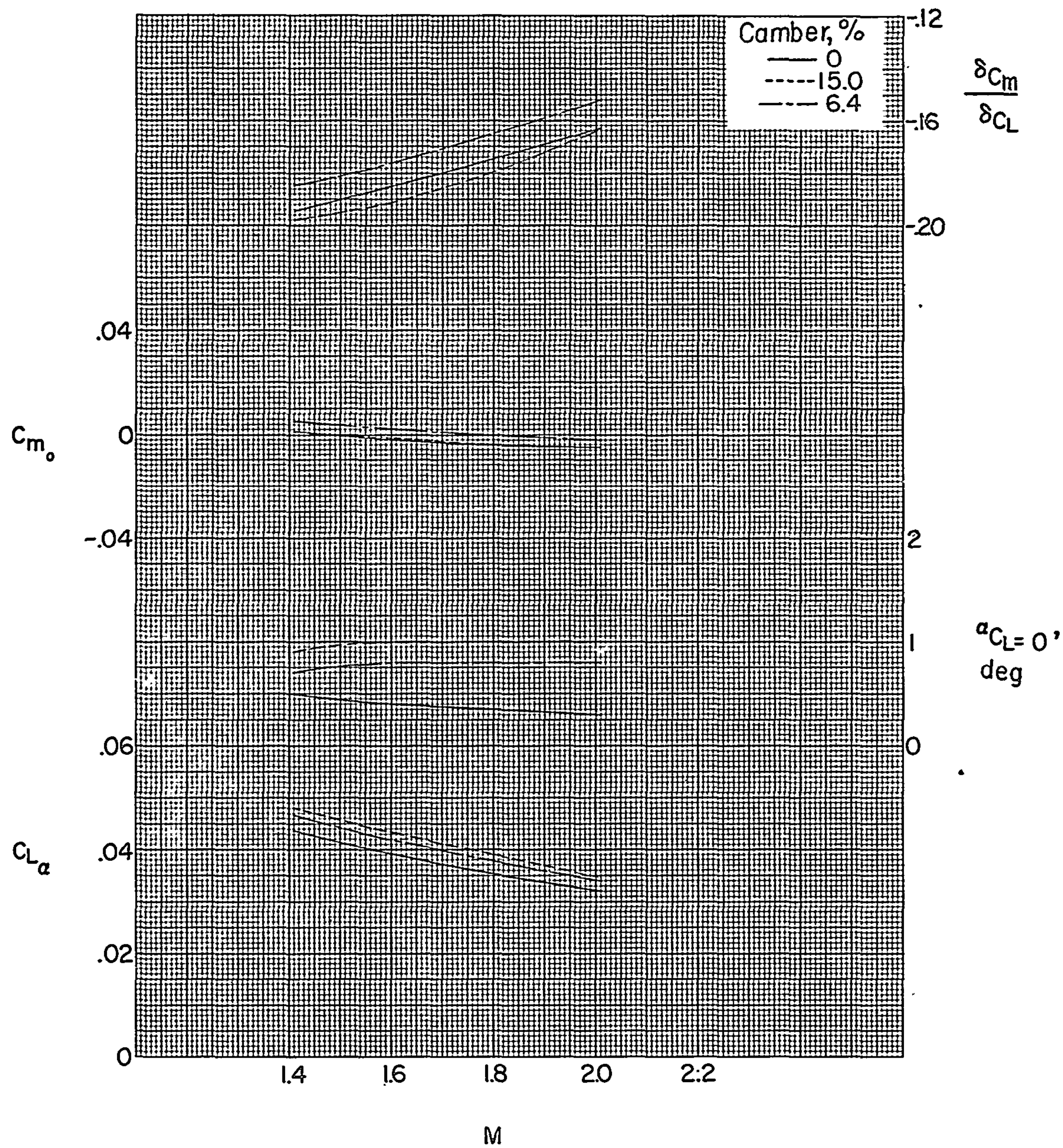

Figure 7.- Effects of camber on the variation with Mach number of longitudinal parameters.

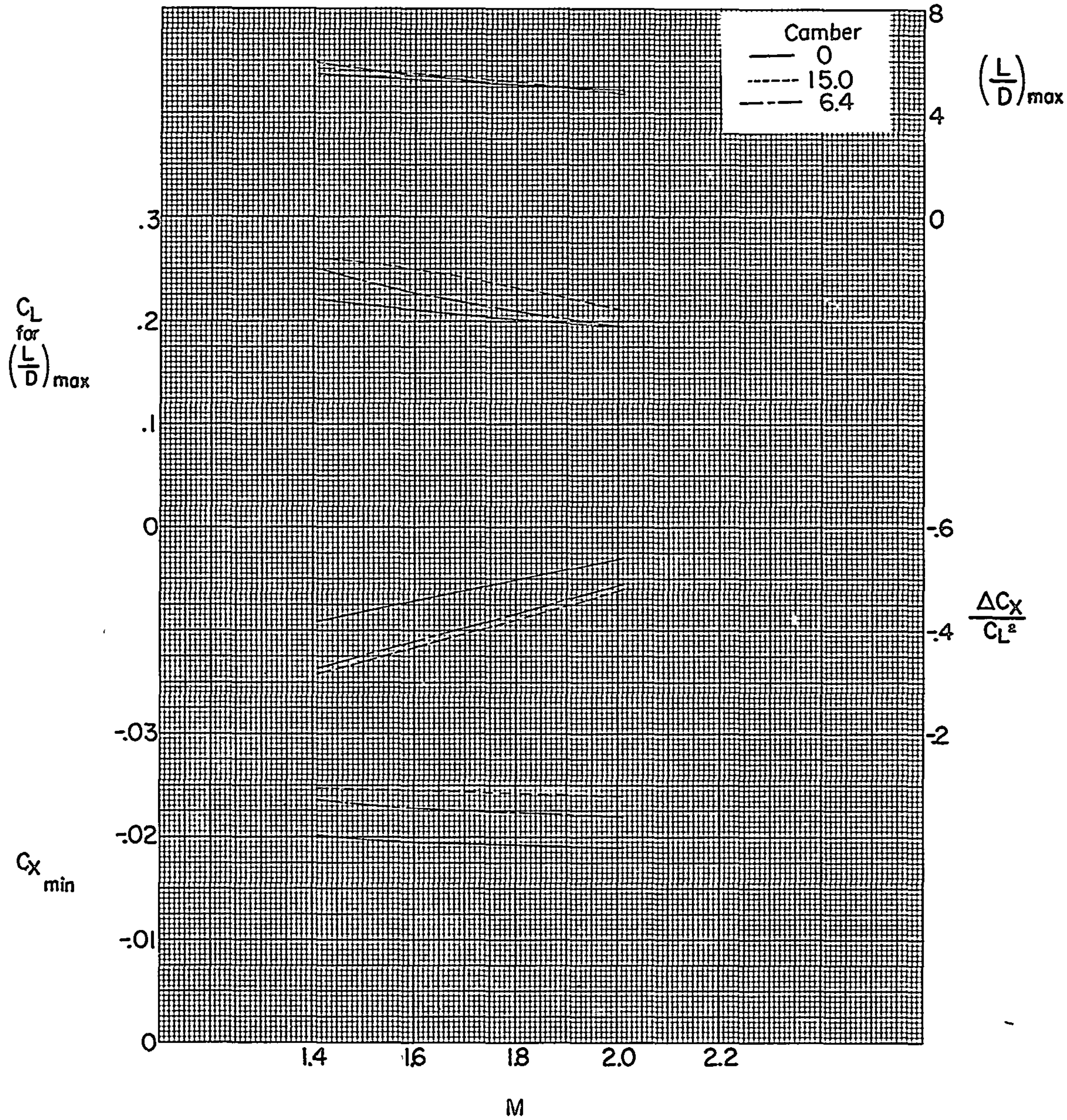

Figure 7.- Concluded.

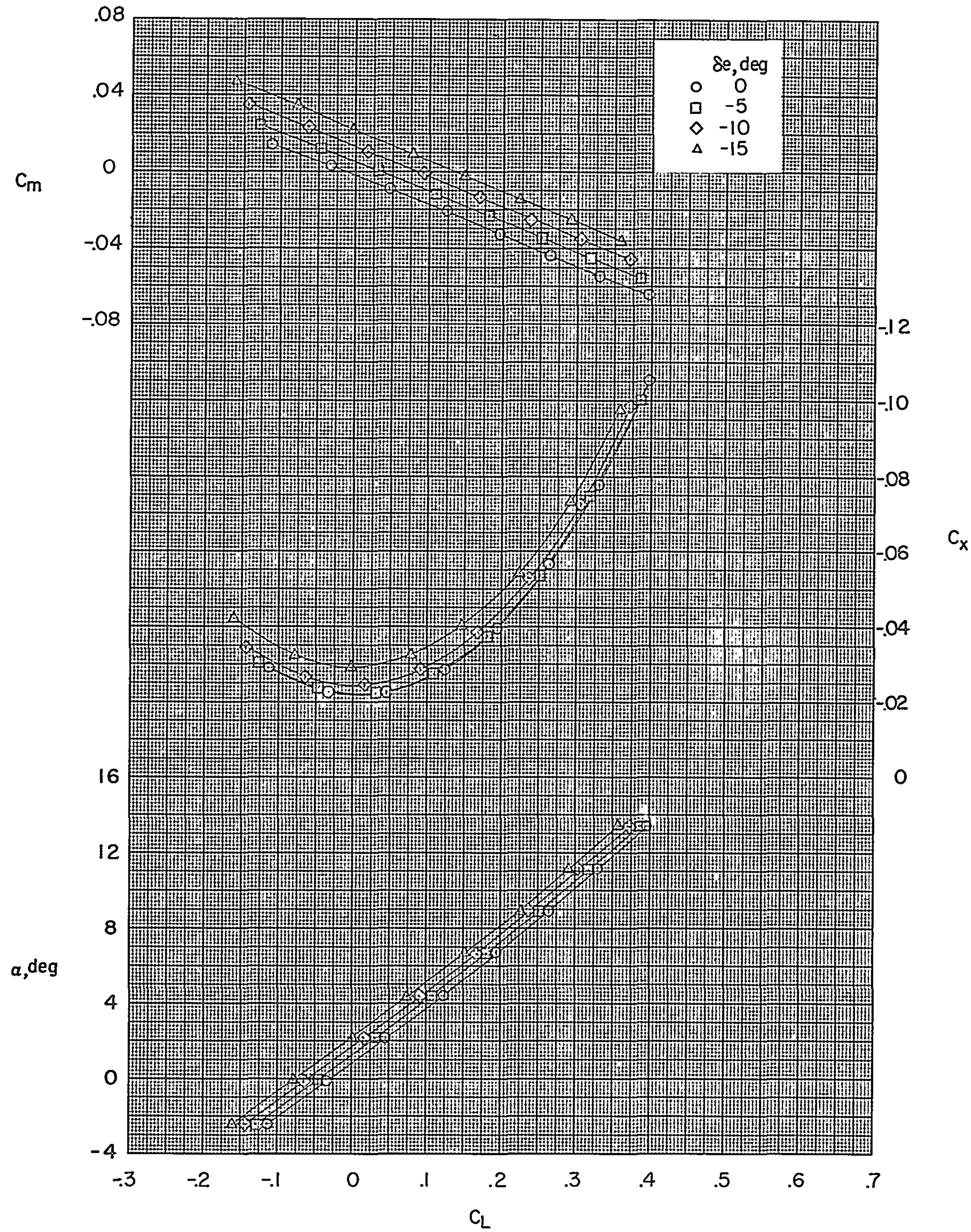

Figure 8.- Effects of elevon deflection on aerodynamic characteristics in pitch. 6.4 percent wing camber; M = 2.01.

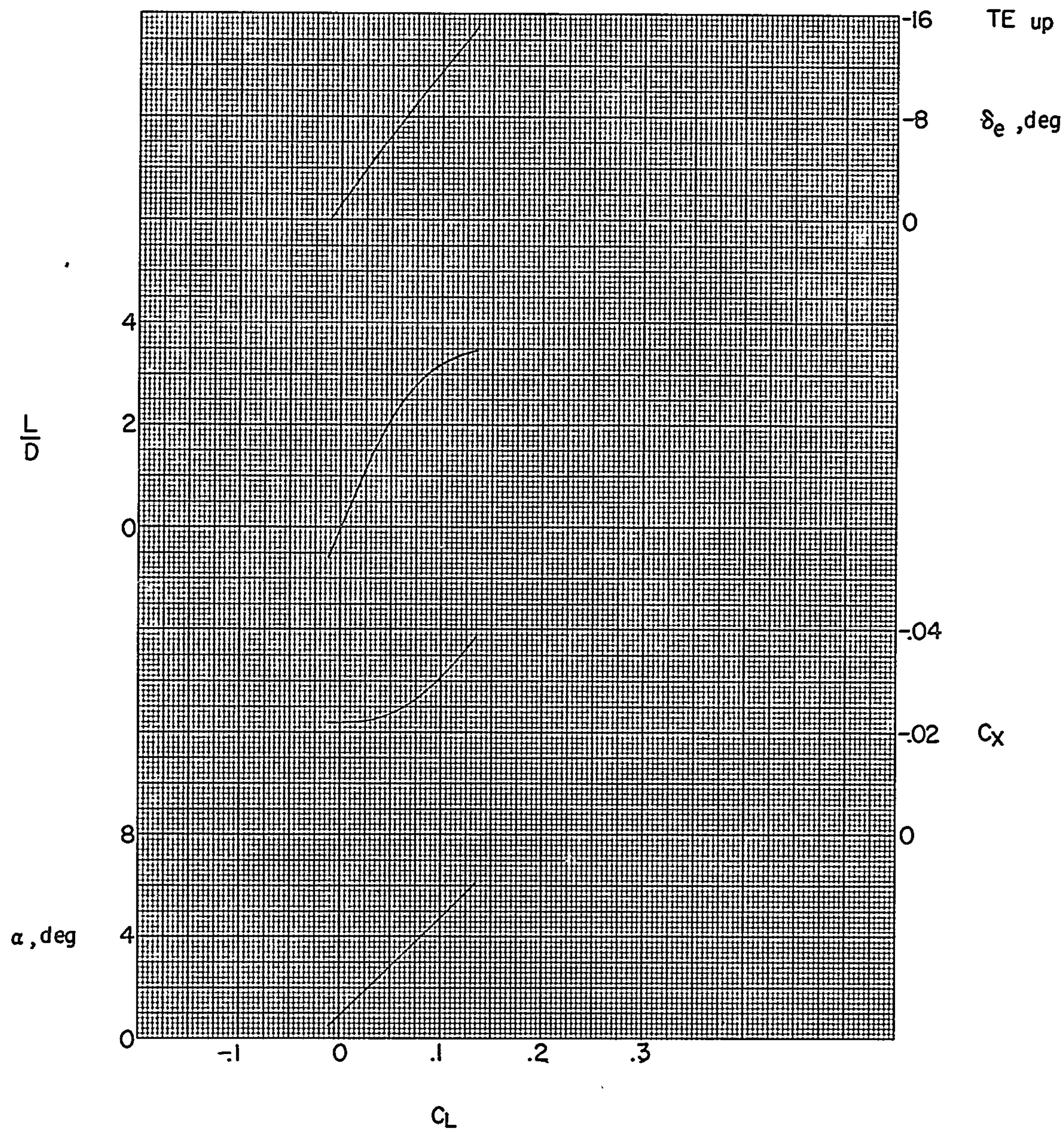

Figure 9.- Longitudinal trim characteristics. 6.4 percent wing camber; M = 2.01.

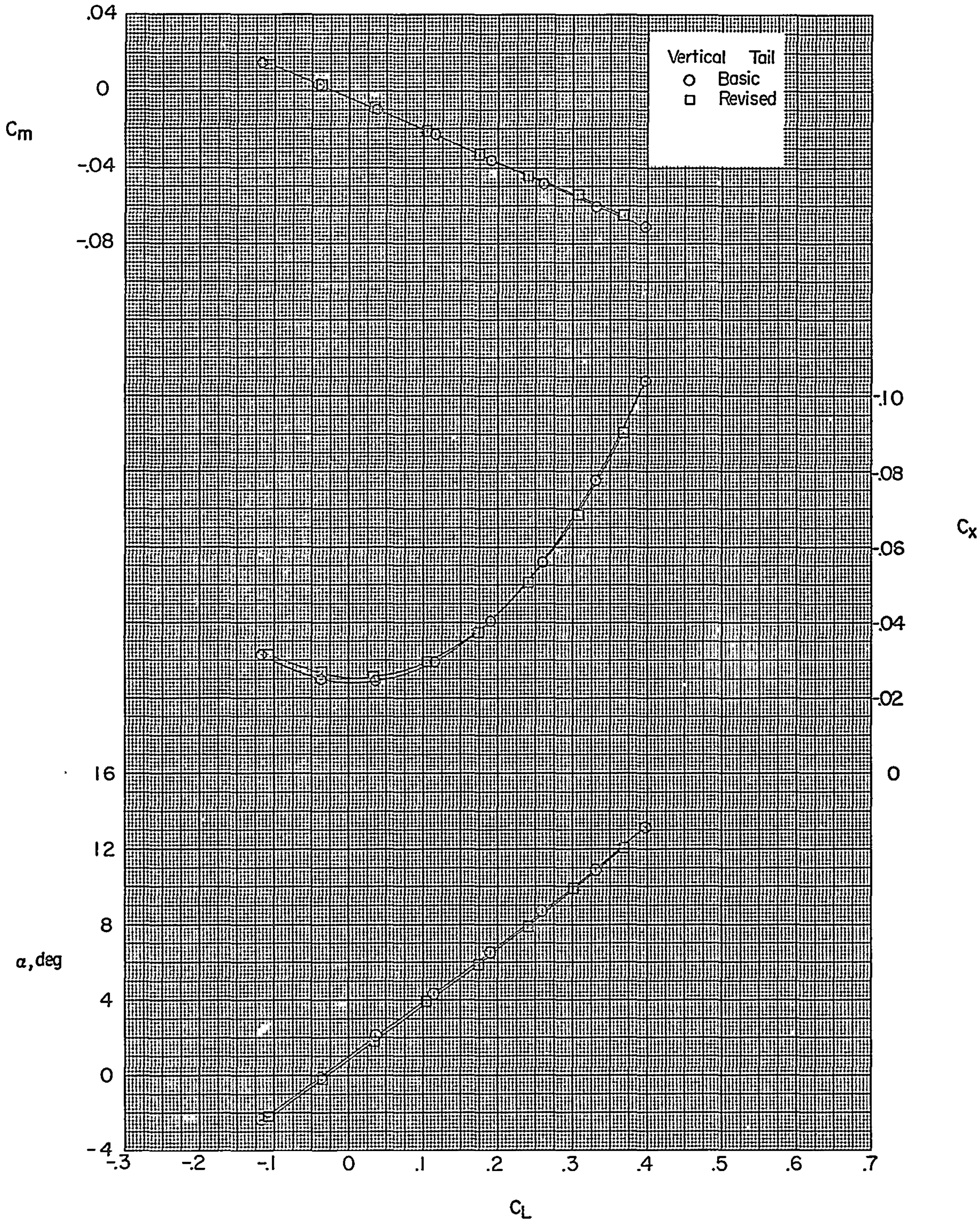

Figure 10.- Effects of vertical tail on aerodynamic characteristics in pitch. 6.4 percent wing camber; M = 2.01.

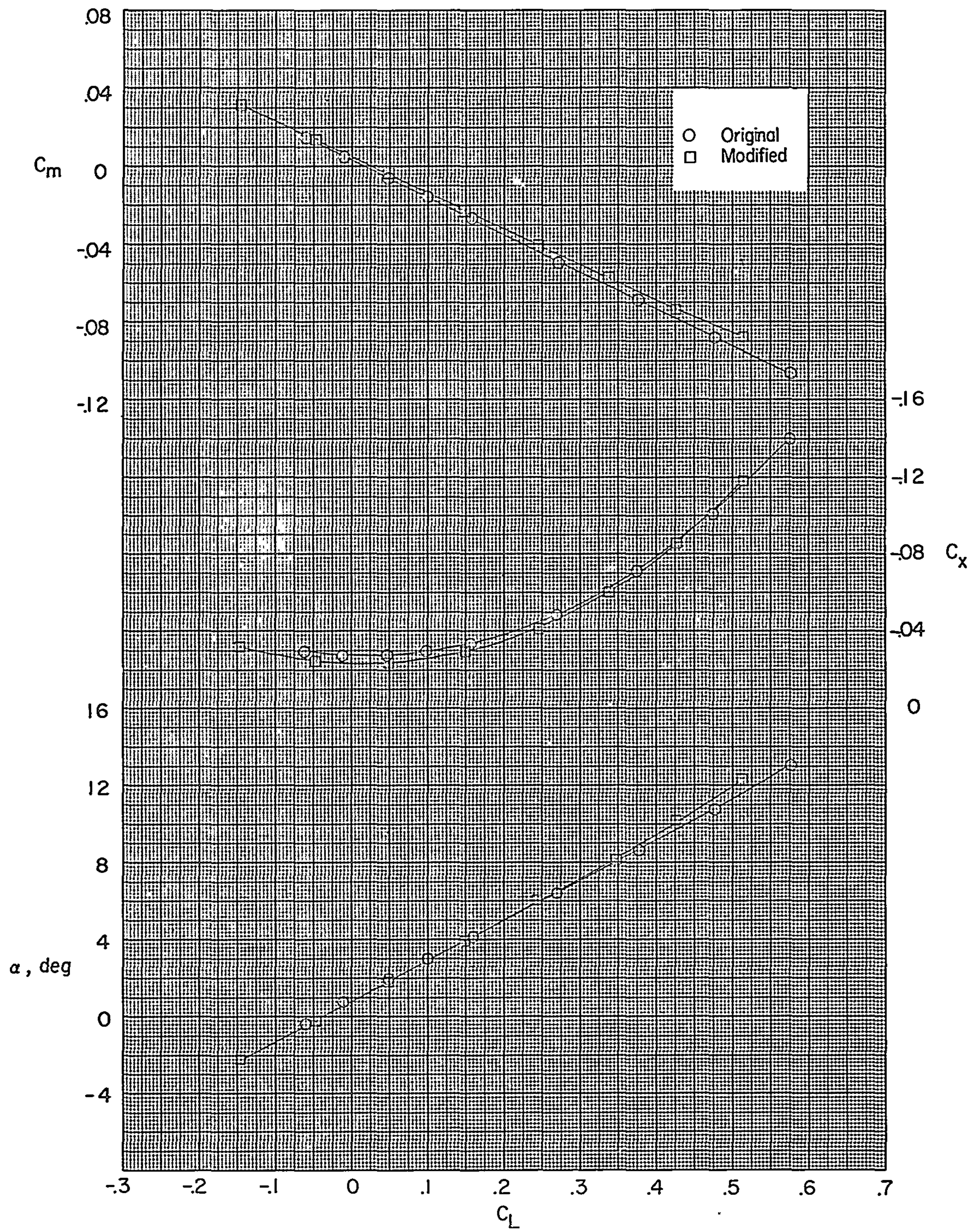

(a) M = 1.41.

Figure 11.- Effects on the longitudinal aerodynamic characteristics of a canopy modification and the addition of extended fillet and extended nose. 6.4 percent wing camber.

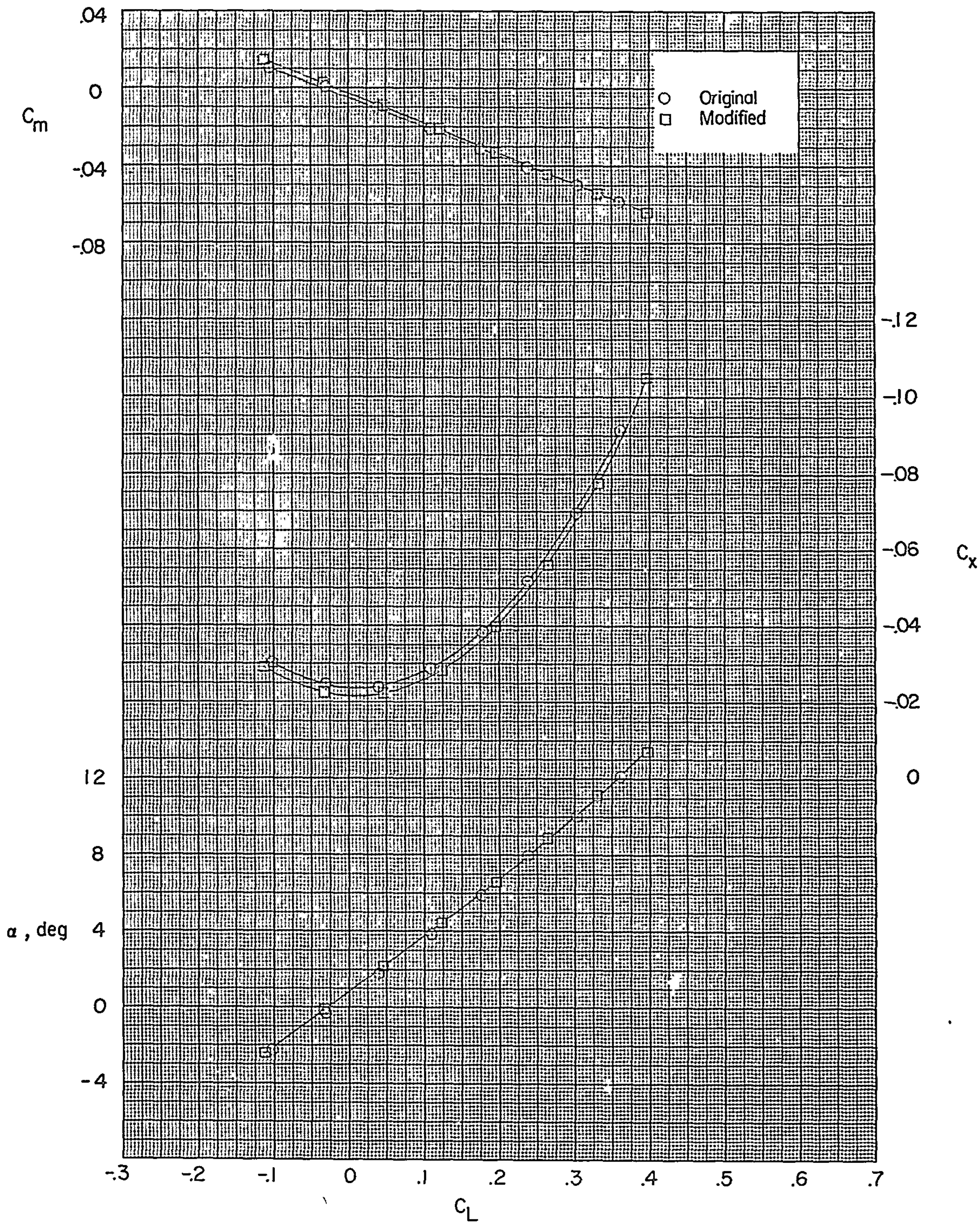

(b) M = 2.01.

Figure 11.- Concluded.

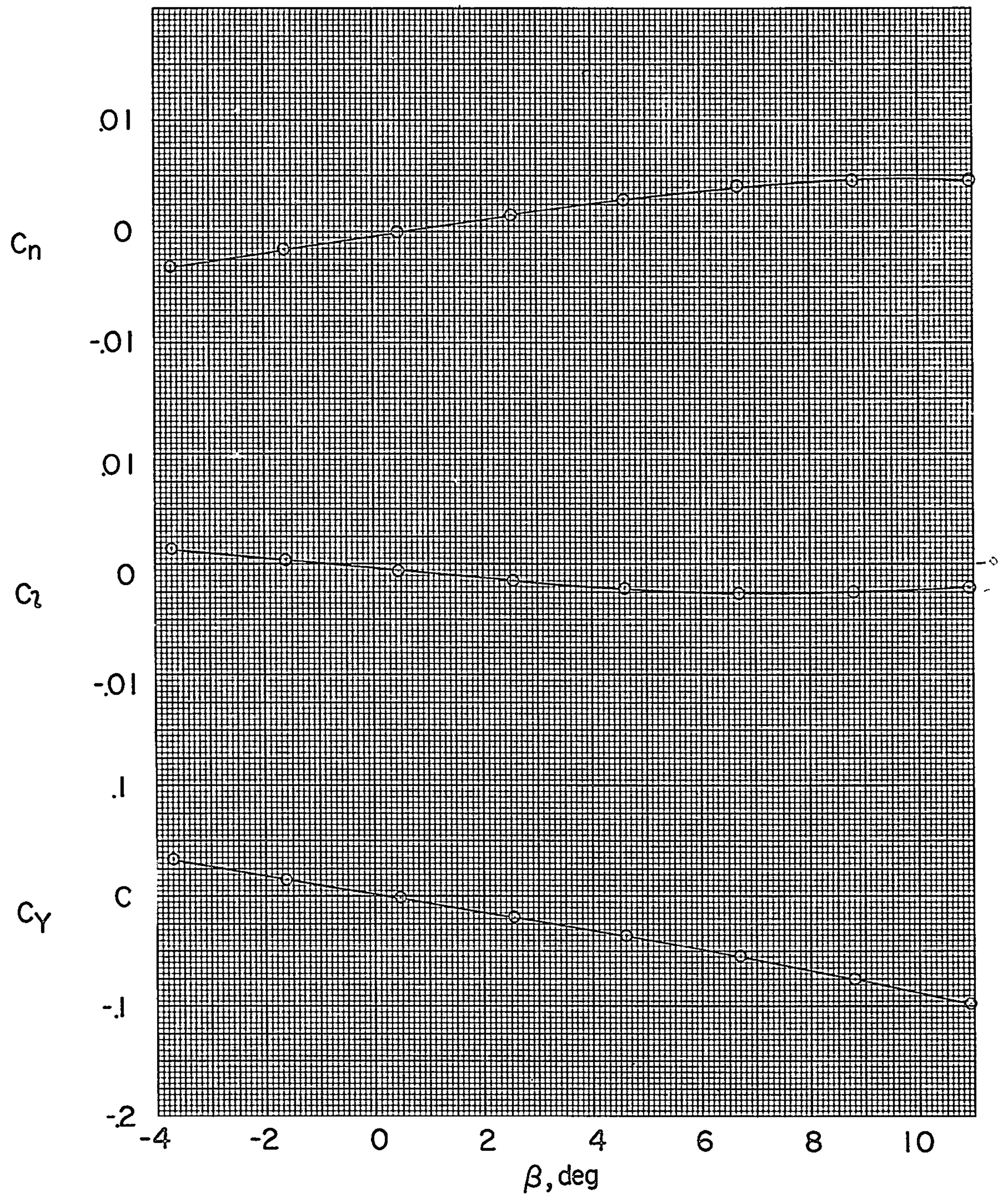

Figure 12.- Aerodynamic characteristics in sideslip. Basic vertical tail; 6.4 percent wing camber; $\alpha = 1.5^{\circ}$; M = 1.61.

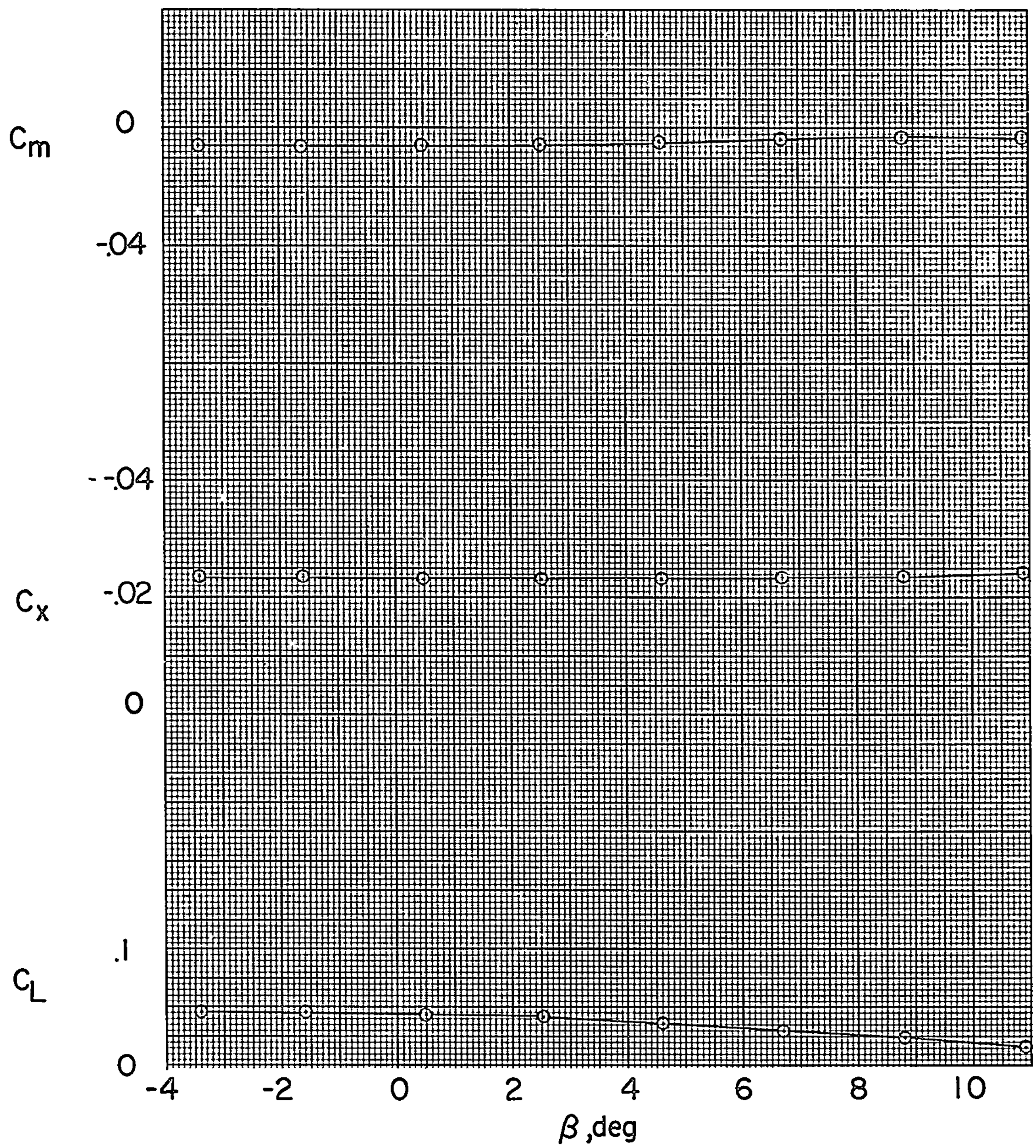

Figure 12.- Concluded.

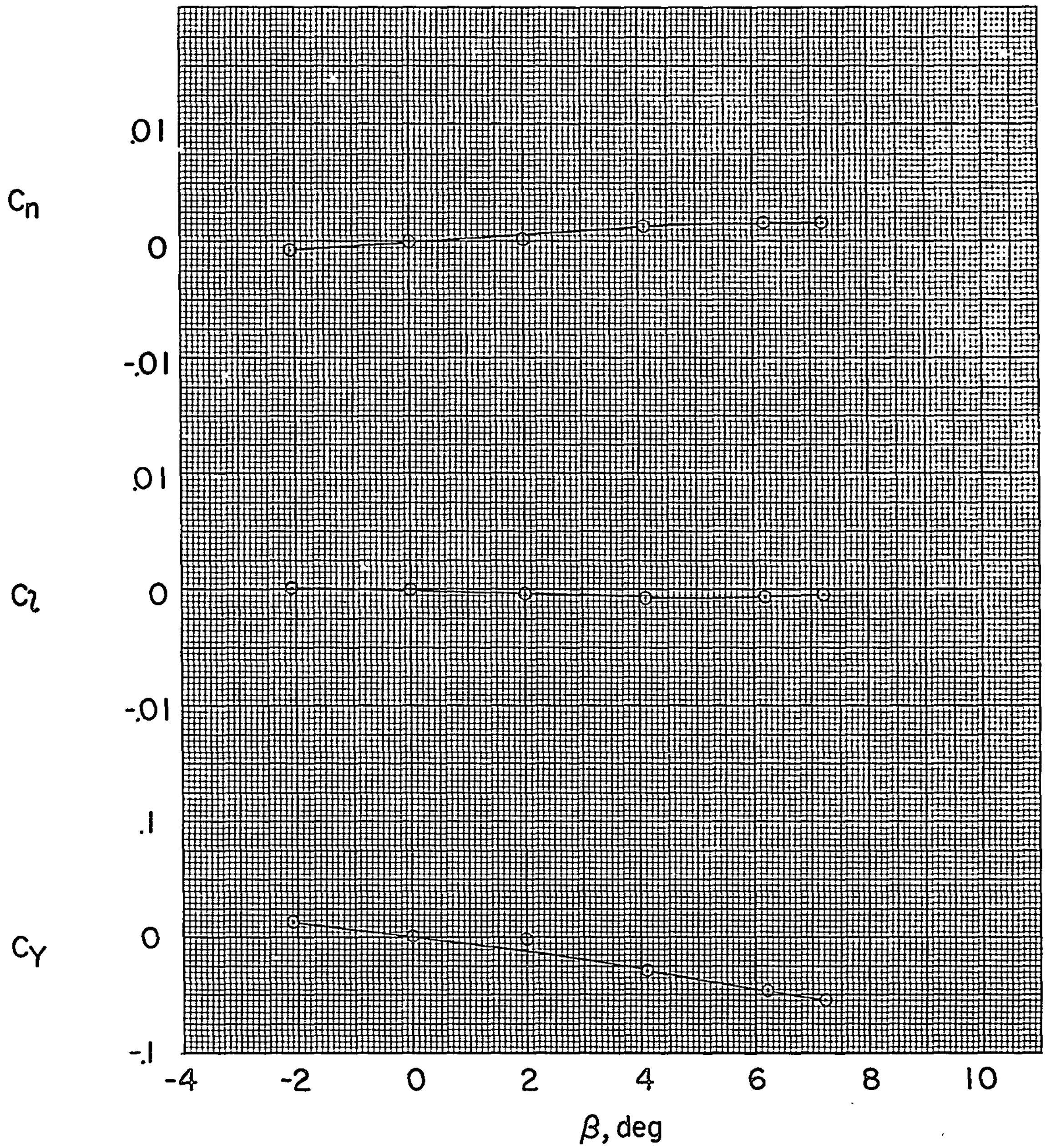

Figure 13.- Aerodynamic characteristics in sideslip. Basic vertical tail; 6.4 percent wing camber; $\alpha = 1.5^{\circ}$; $M = 2.01$.

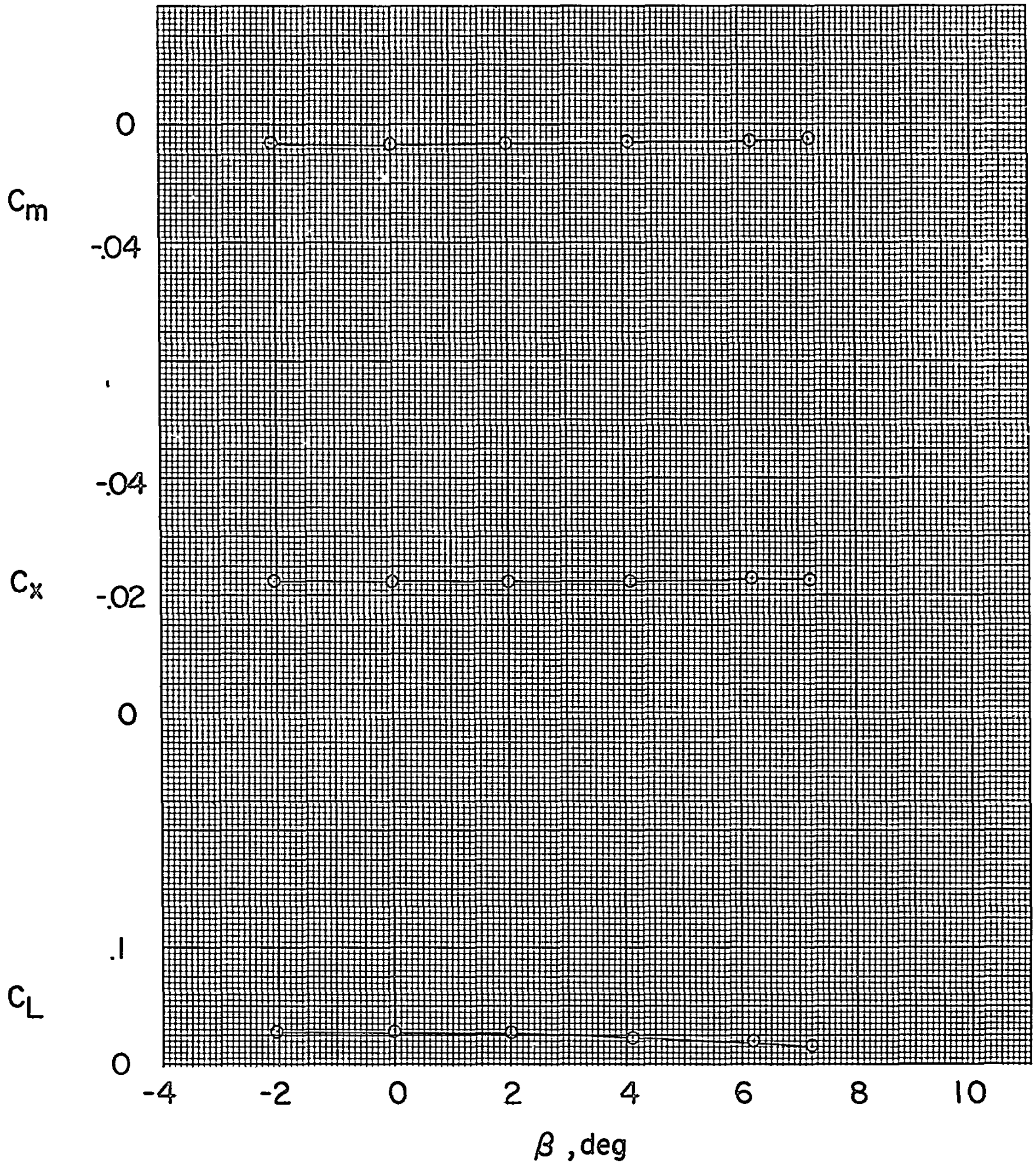

Figure 13.- Concluded.

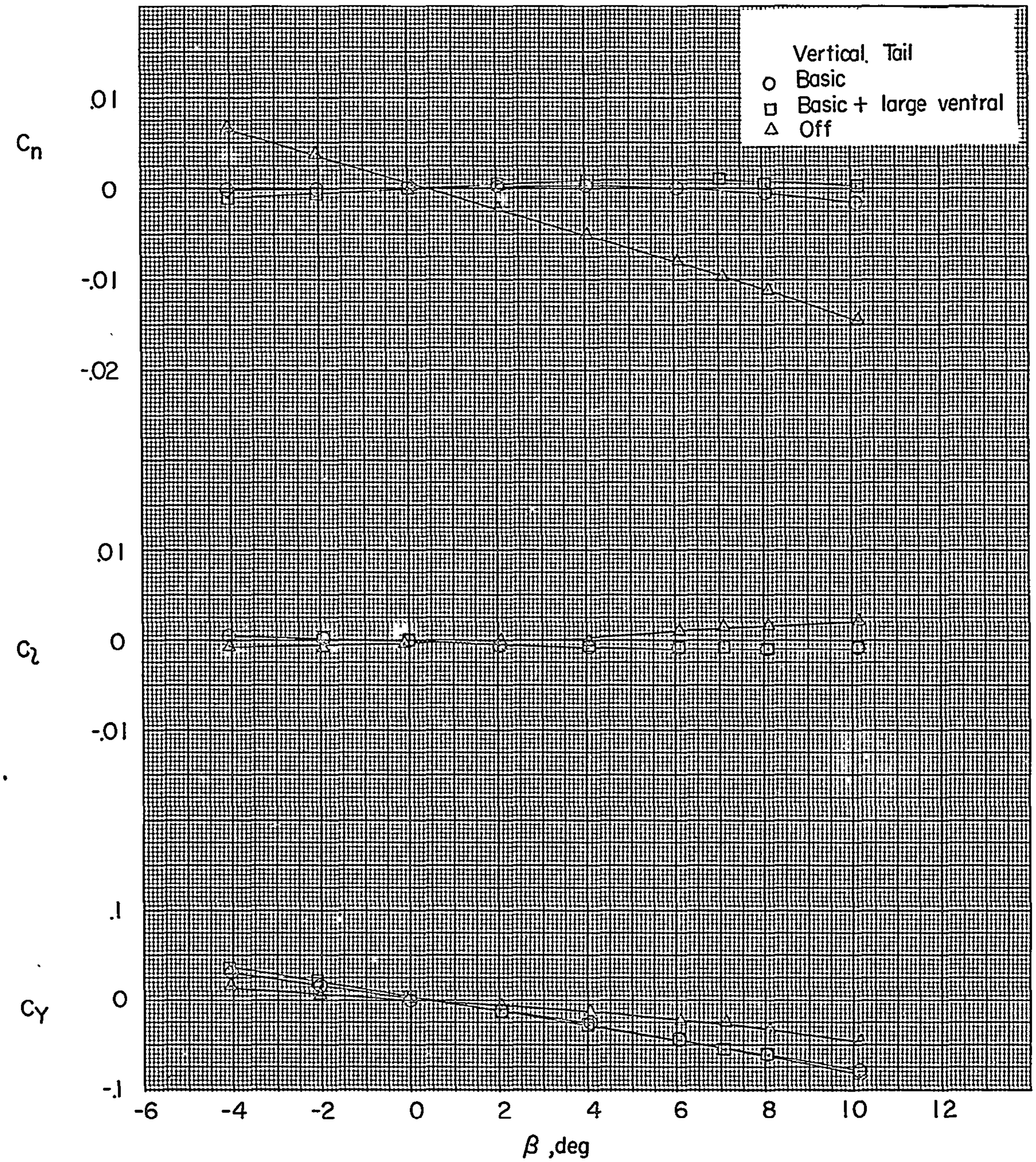

Figure 14.- Effect of large ventral fin on aerodynamic characteristics in sideslip. 6.4 percent wing camber; $\alpha = 5.7^{\circ}$; $M = 2.01$.

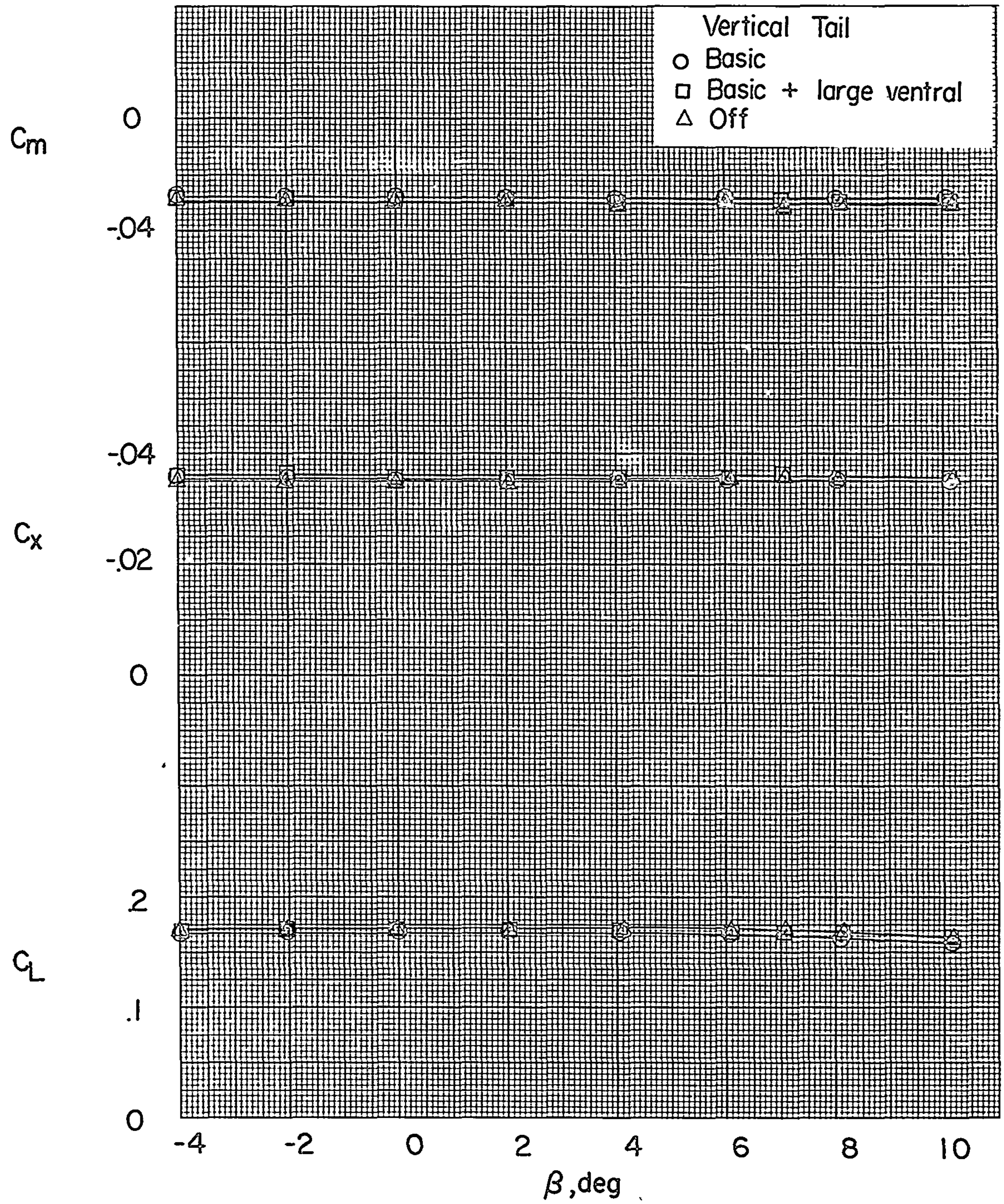

Figure 14.- Concluded.

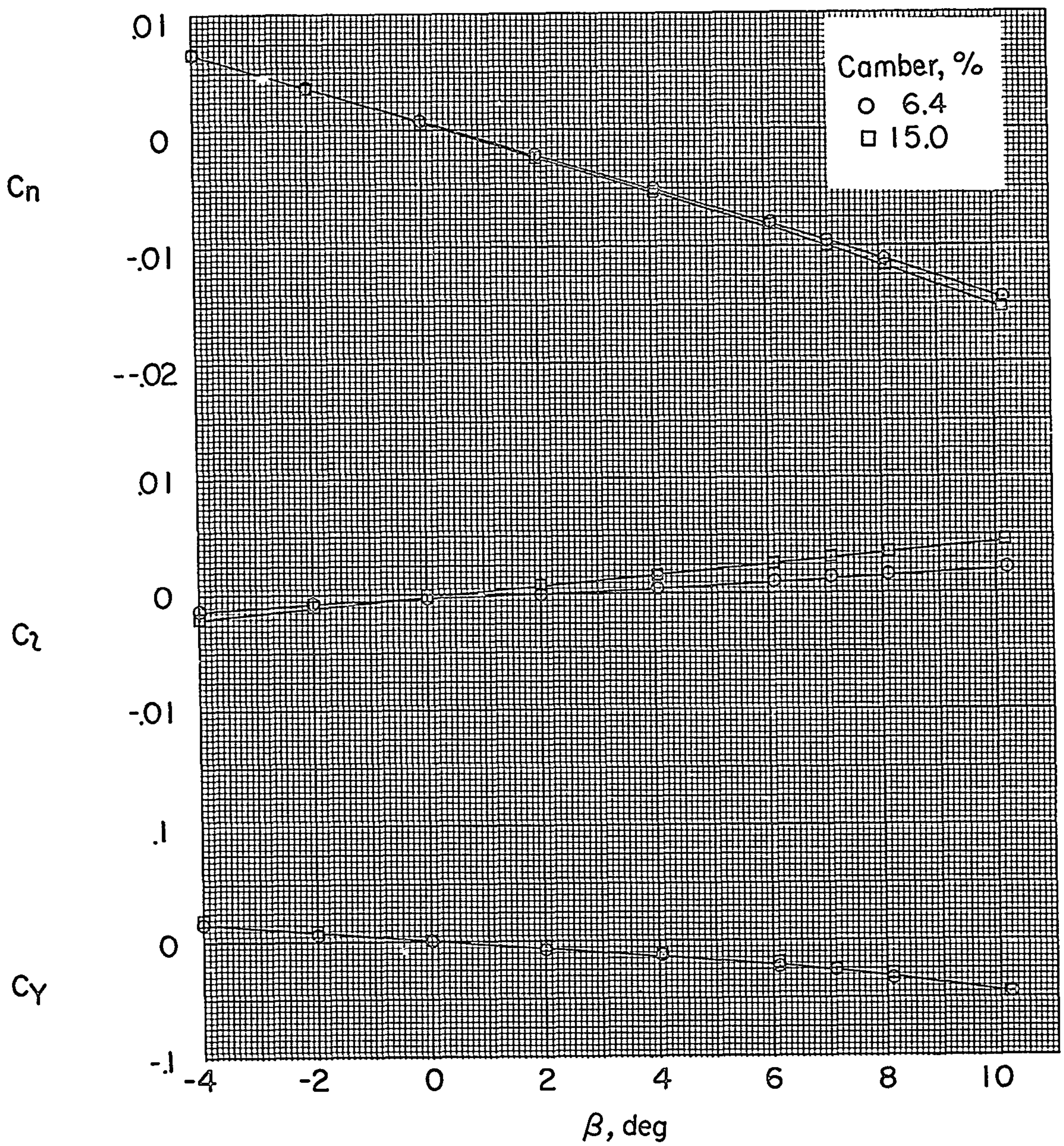

Figure 15.- Effects of wing camber on the aerodynamic characteristics in sideslip. Vertical tail off; $\alpha = 5.6^\circ$; M = 2.01.

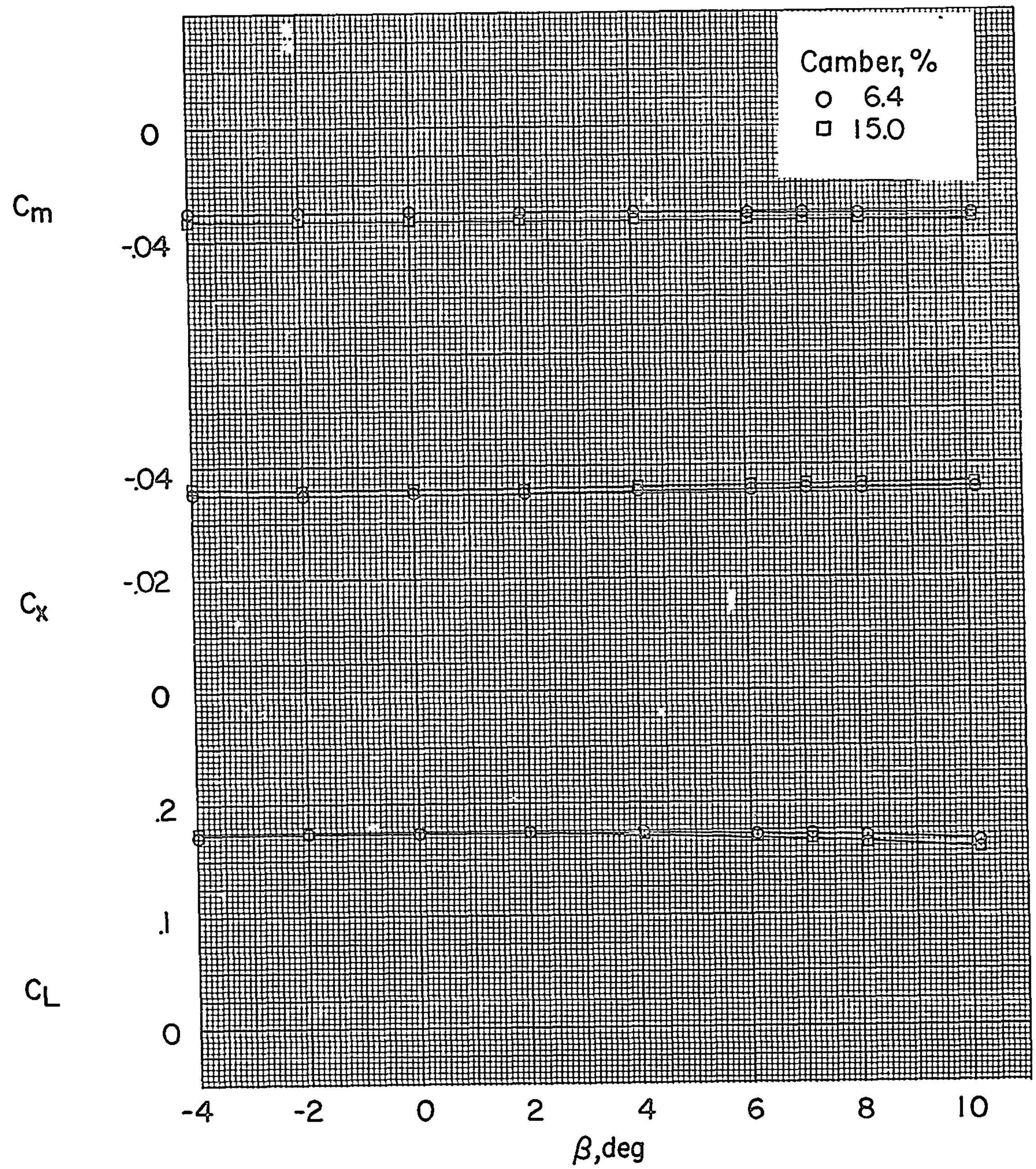

Figure 15.- Concluded.

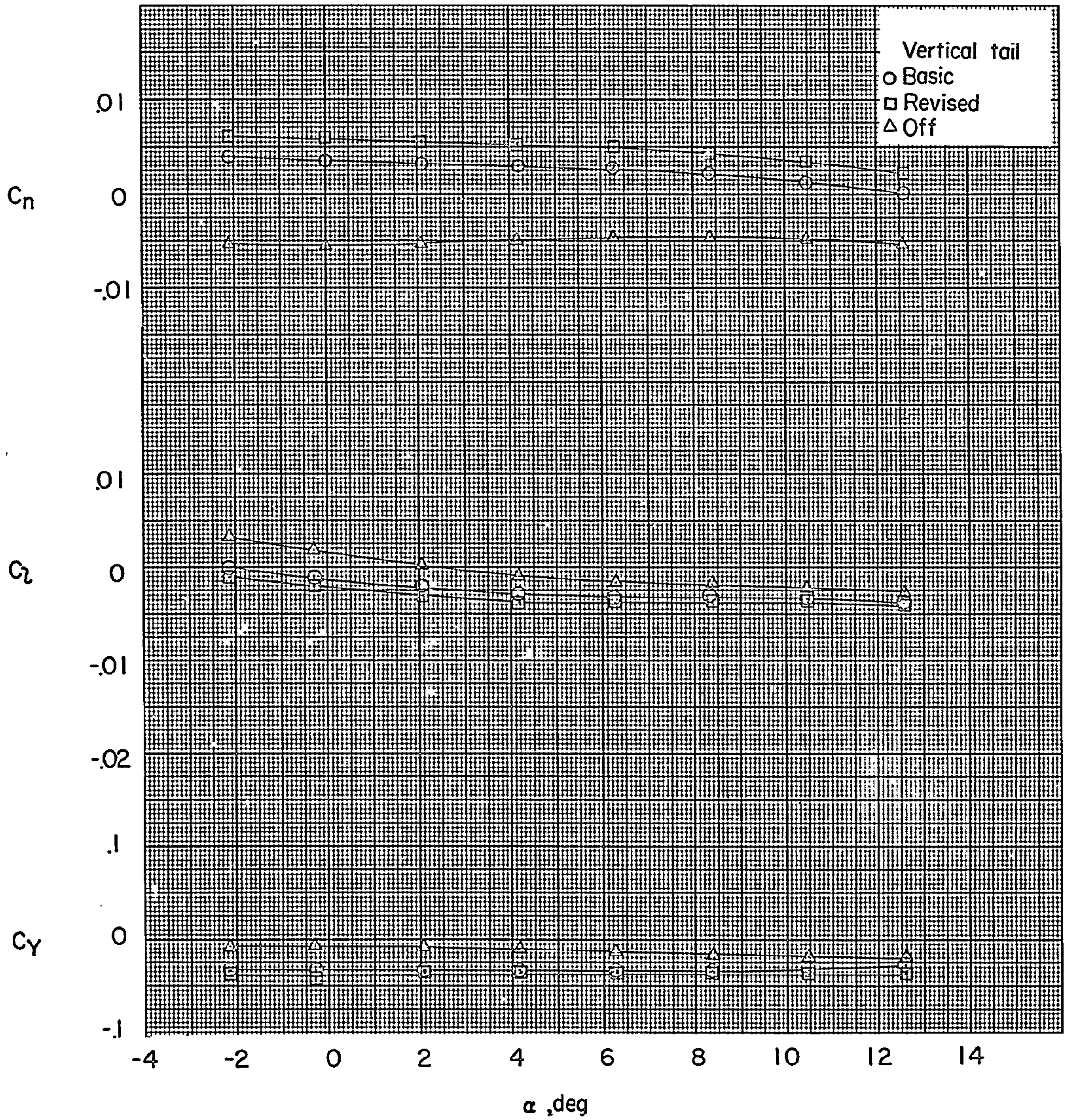

Figure 16.- Effects of angle of attack and vertical tail on lateral characteristics. 6.4 percent wing camber; $\beta = 4^{\circ}$; M = 1.41.

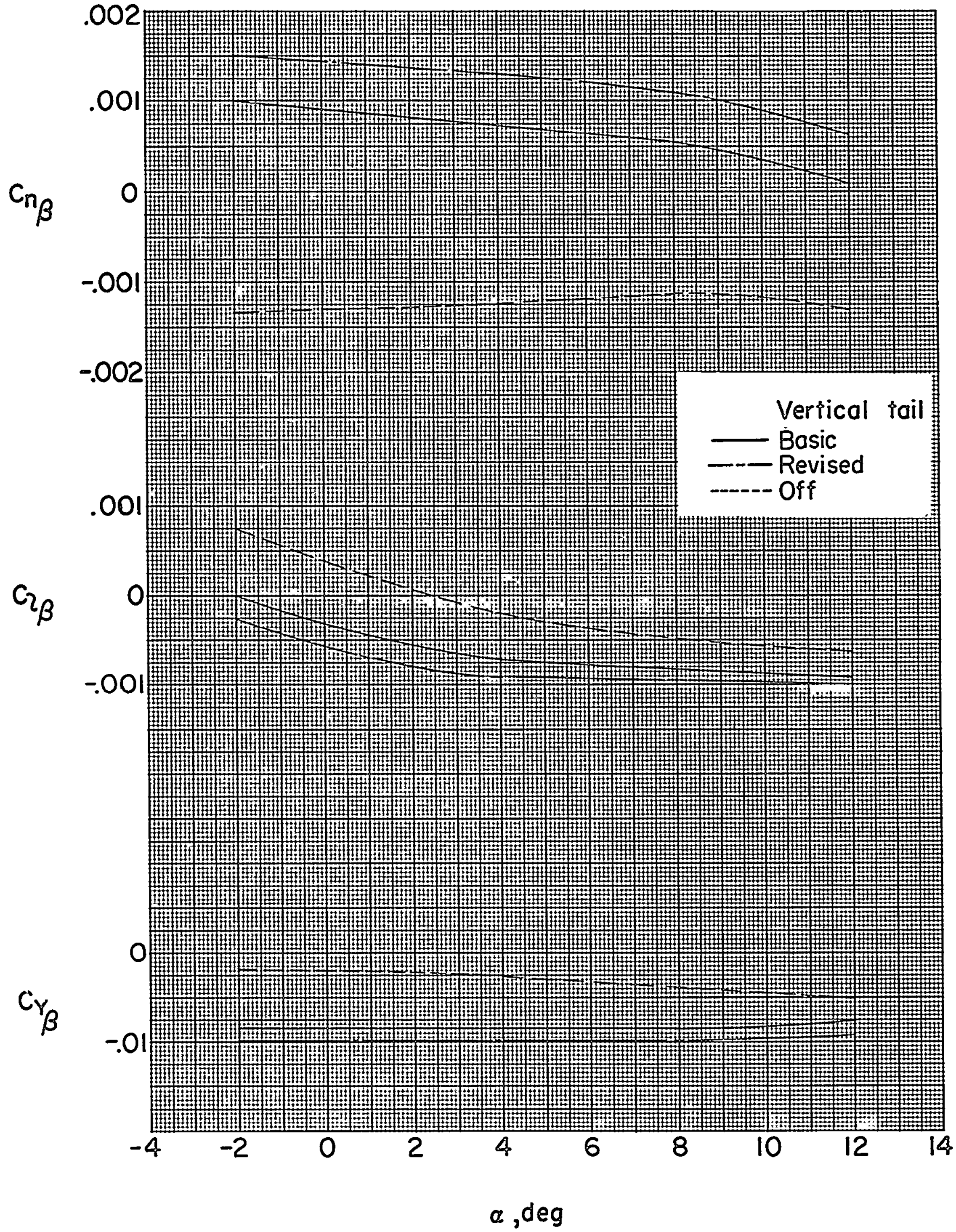

Figure 17.- Effect of vertical tail on the variation of the sideslip derivatives with angle of attack. 6.4 percent camber; M = 1.41.

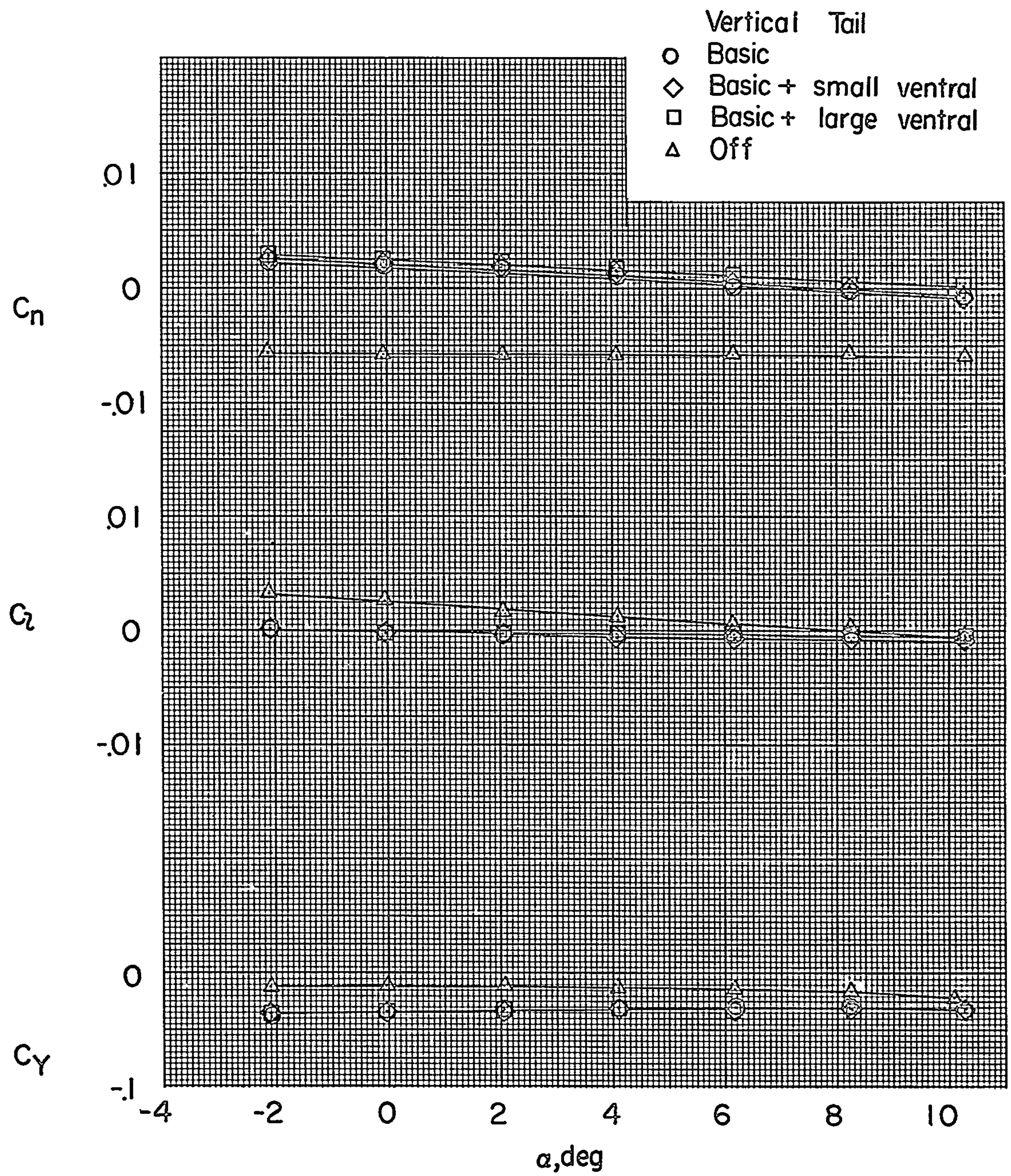

Figure 18.- Effects of angle of attack and ventral fins on lateral characteristics. $\beta = 4^{\circ}$; 6.4 percent wing camber; M = 2.01.

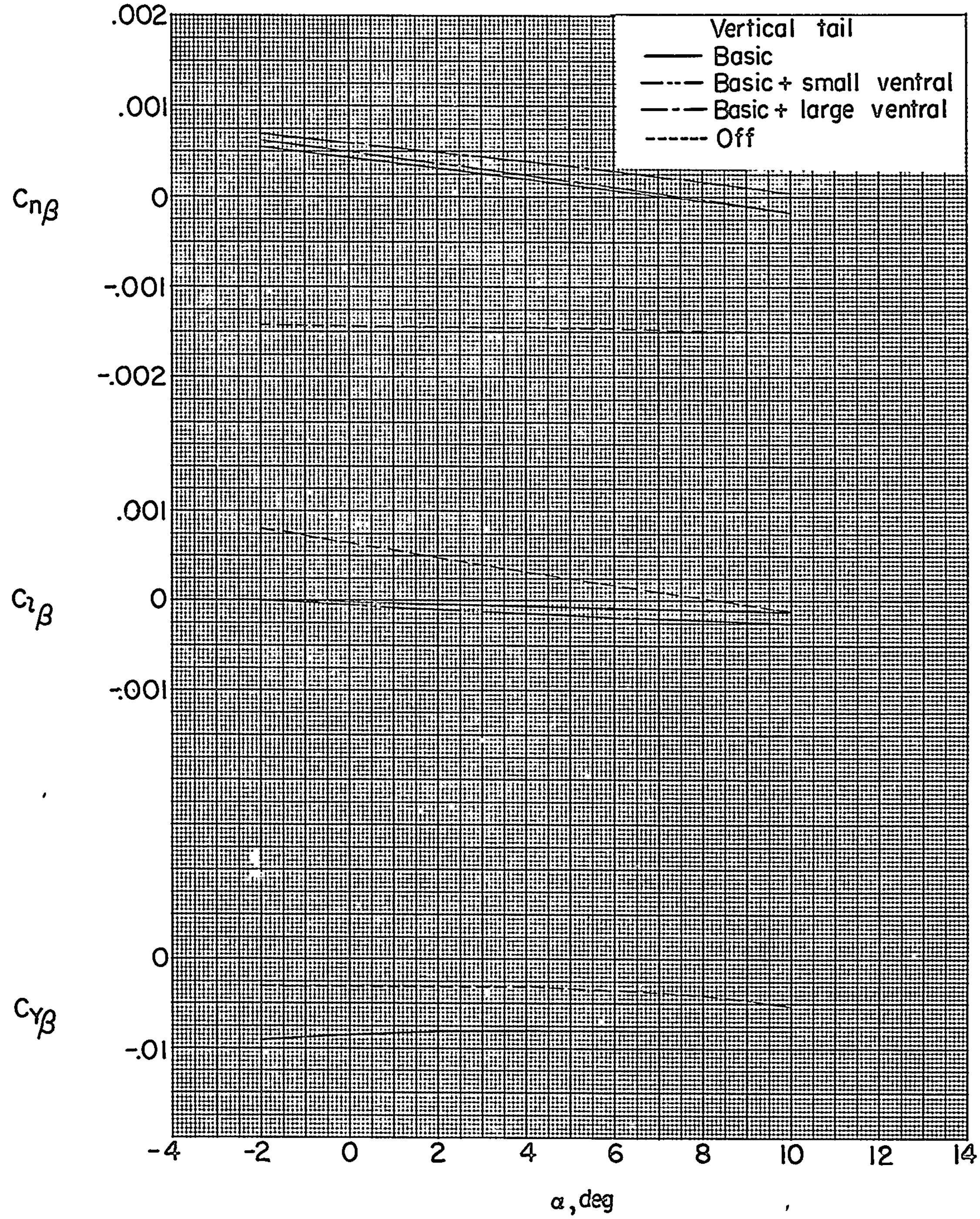

Figure 19.- Effects of ventral fins on the variation of the sideslip derivatives with angle of attack. 6.4 percent wing camber; M = 2.01.

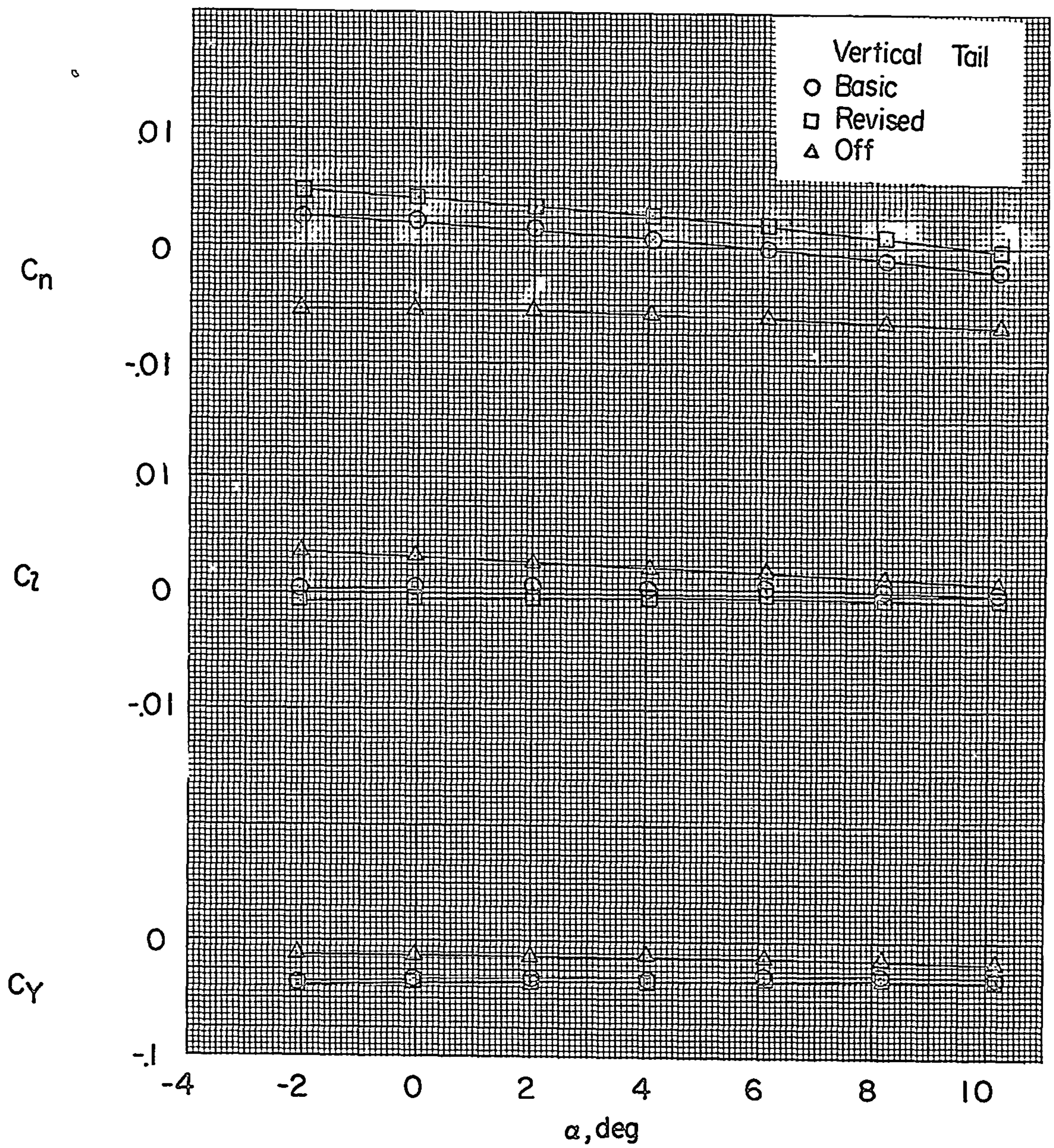

Figure 20.-Effects of angle of attack and revised vertical tail on the lateral characteristics. $\beta = 4^{\circ}$; 15.0 percent wing camber; M = 2.01.

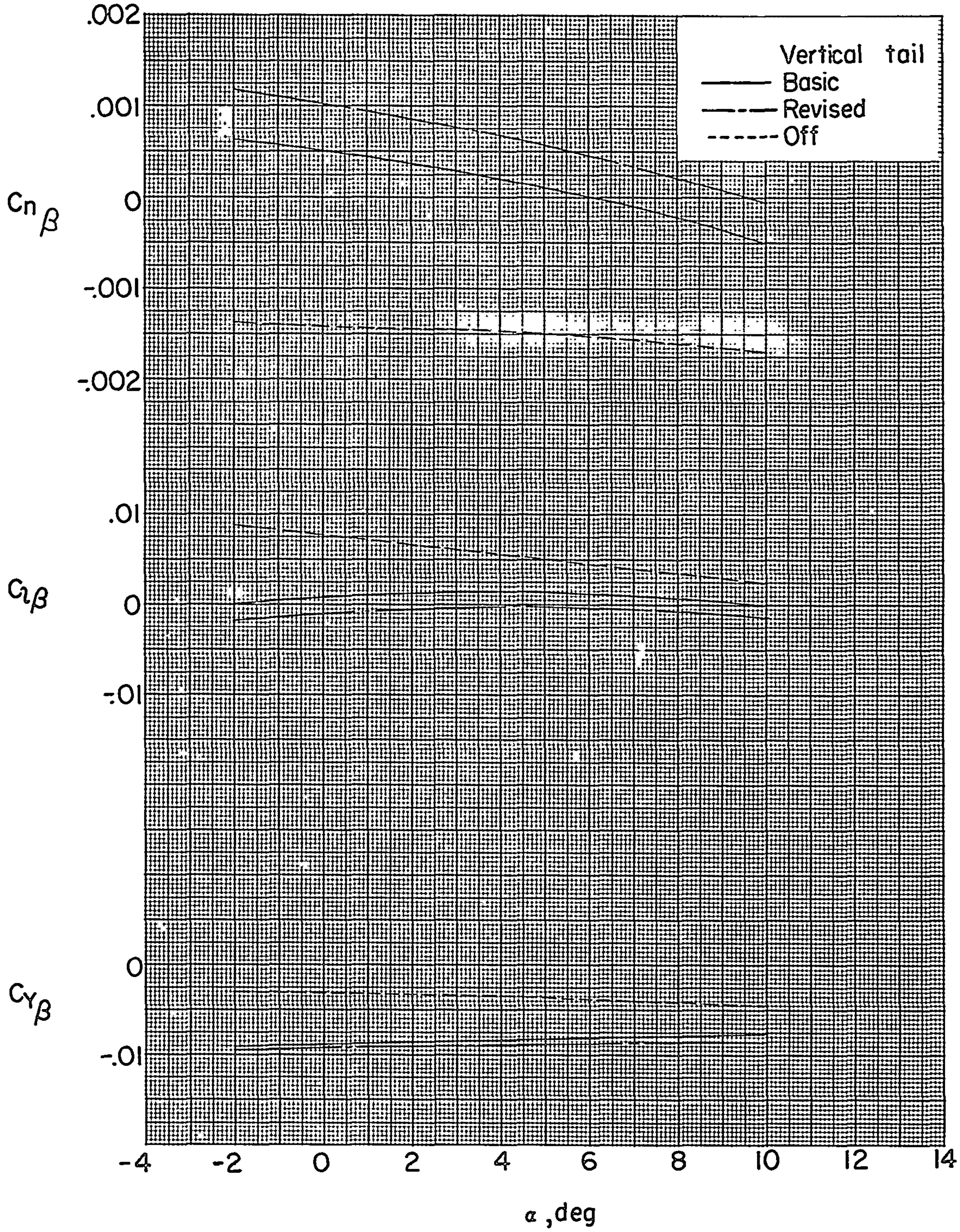

Figure 21.- Effect of vertical tail on the variation of the sideslip derivatives with angle of attack. 15.0 percent wing camber; M = 2.01.

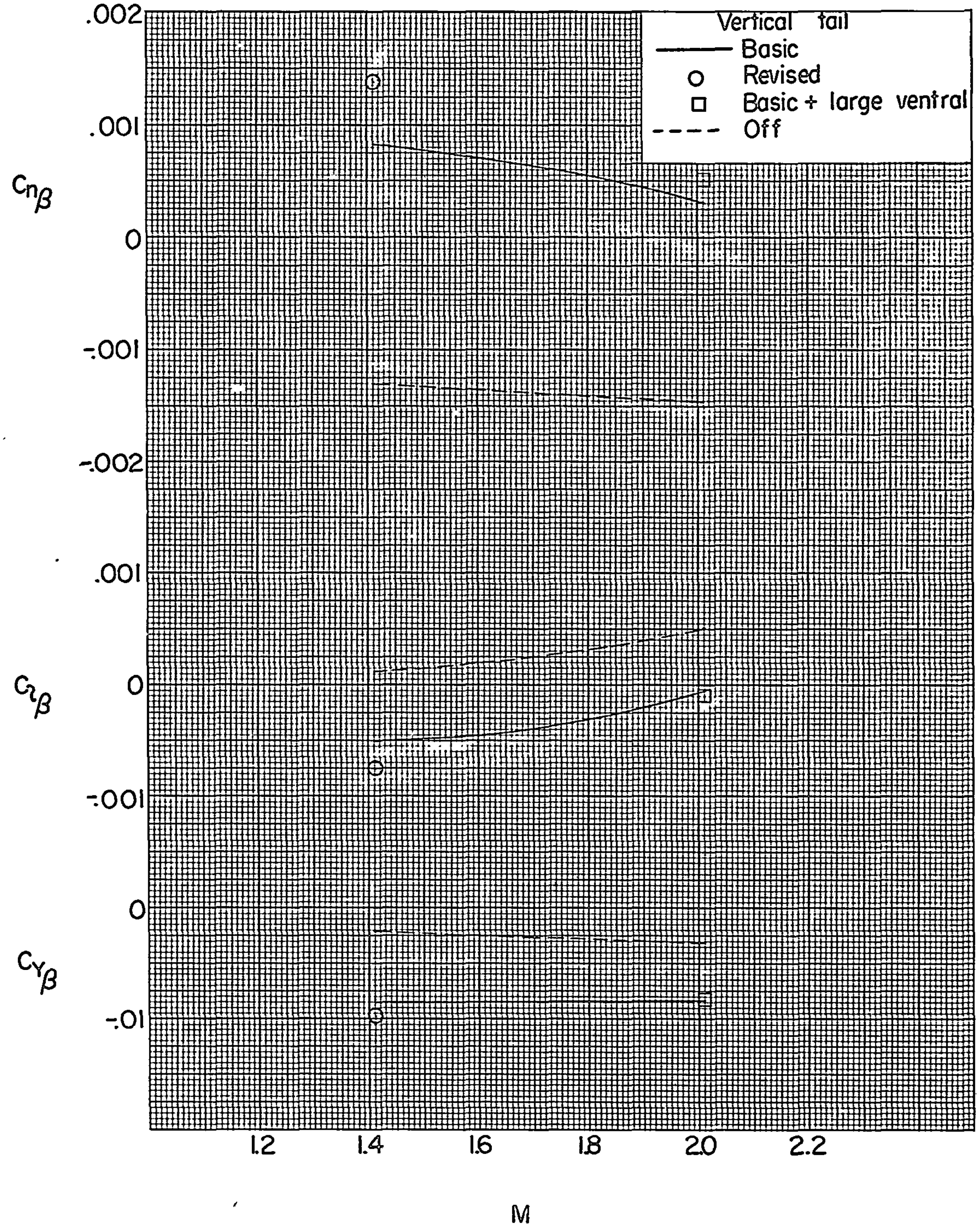

Figure 22.- Variation of sideslip derivatives with Mach number for various vertical tail arrangements. $\alpha = 1.5^{\circ}$; 6.4 percent wing camber.